May 2026

DEVELOPMENT OF A COMPUTATIONAL FRAMEWORK FOR STATEWIDE COUPLED SURFACE WATER AND GROUNDWATER MODELING

NM WRRI Technical Completion Report No. 412

Huidae Cho
Abdullah Azzam

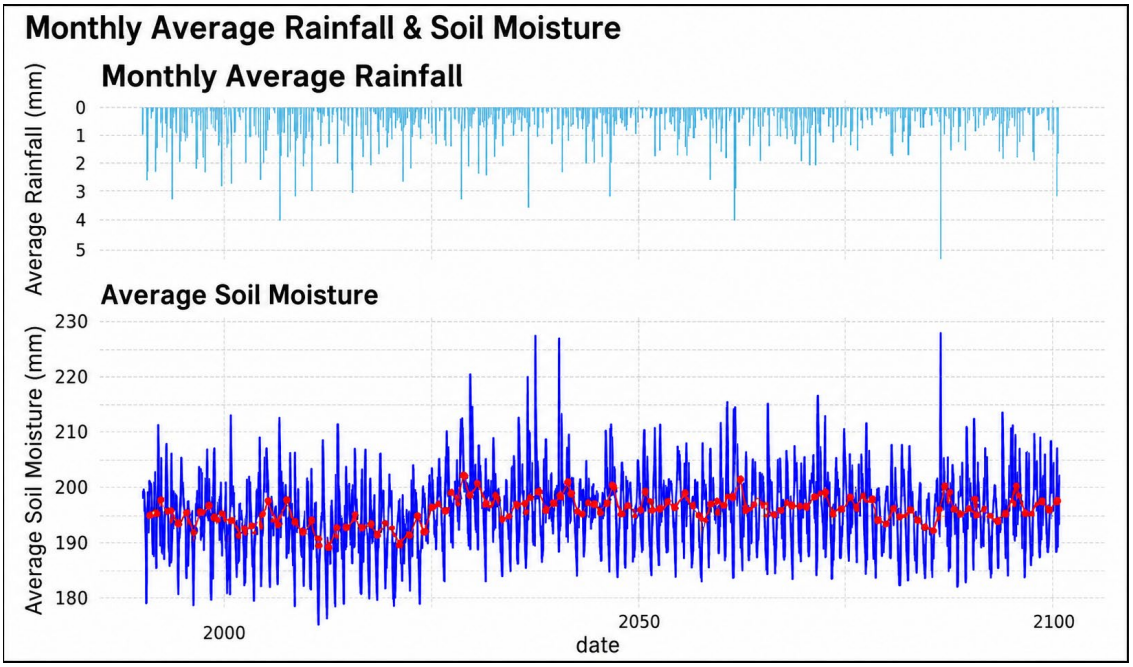

Average Monthly Soil Moisture for the Simulation Period with Monthly 12-Month Moving Average in Red

New Mexico Water Resources Research Institute
New Mexico State University
MSC 3167, P.O. Box 30001
Las Cruces, New Mexico 88003-0001
(575) 646-4337 email: nmwrri@nmsu.edu

DEVELOPMENT OF A COMPUTATIONAL FRAMEWORK FOR STATEWIDE COUPLED SURFACE WATER AND GROUNDWATER MODELING

By

Huidae Cho, Associate Professor
Abdullah Azzam, Graduate Student

Department of Civil Engineering
New Mexico State University

TECHNICAL COMPLETION REPORT
Account Number 07017
Technical Completion Report #412

May 2026

New Mexico Water Resources Research Institute
in cooperation with the
Department of Civil Engineering
New Mexico State University

The research on which this report is based was financed in part by the U.S. Department of the Interior, Geological Survey, through the New Mexico Water Resources Research Institute. This material is based upon work supported by the U.S. Geological Survey under Grant/Cooperative Agreement No. G21AP10635, along with additional funding by the New Mexico Legislature, through the NM WRRI.

Page Intentionally Left Blank

DISCLAIMER

The purpose of the NM Water Resources Research Institute (NM WRRI) technical reports is to provide a timely outlet for research results obtained on projects supported in whole or in part by the institute. Through these reports the NM WRRI promotes the free exchange of information and ideas and hopes to stimulate thoughtful discussions and actions that may lead to resolution of water problems. The NM WRRI, through peer review of draft reports, attempts to substantiate the accuracy of information contained within its reports, but the views and conclusions contained in this document are those of the authors and should not be interpreted as representing the opinions or policies of the U.S. Geological Survey. Mention of trade name or commercial products does not constitute their endorsement by the U.S. Geological Survey. This manuscript is submitted for publication with the understanding that the United States Government is authorized to reproduce and distribute reprints for Governmental purposes.

ABSTRACT

New Mexico, one of the fastest-warming states in the United States, faces increasing challenges in managing water resources because of declining snowpack and intensified groundwater extraction. To address these challenges, we developed a high-resolution, fully automated hydrologic modeling framework that couples the Variable Infiltration Capacity (VIC) surface water model with the MODFLOW 6 (MF6) groundwater model. This coupled hydrologic modeling framework, called VIC-MF6, can be used to simulate surface-subsurface hydrologic interactions across New Mexico from 1940 to 2100 using observed and Coupled Model Intercomparison Project Phase 6 (CMIP6)-projected climate data at a 1/32° resolution. It includes modules for parameter downscaling, data conversion, and model synchronization via the MF6 Application Programming Interface (API) based on the eXtended Model Interface (XMI), allowing monthly exchange of baseflow and groundwater discharge. The model was applied to the domain of the Rio Grande Transboundary Integrated Hydrologic Model (RGTIHM), demonstrating scalability, computational efficiency, and physical consistency. Key findings highlight the seasonal dynamics of soil moisture and the long-term trends in groundwater drawdown. Software modifications improved VIC-MF6 compatibility and implemented critical features for MF6 to accommodate the RGTIHM's geological structure within the coupled framework. This study presents the first tightly coupled, statewide hydrologic simulation framework for New Mexico, offering a robust tool for evaluating long-term water availability, drought vulnerability, and sustainable water resources management under variable climatic conditions.

Keywords

New Mexico, Rio Grande Basin, groundwater, surface-subsurface hydrologic coupling, VIC, MODFLOW 6, hydrologic modeling framework, parallelization.

TABLE OF CONTENTS

LIST OF FIGURES

LIST OF TABLES

1. INTRODUCTION

1.1. Background and Motivation

New Mexico, identified as the sixth fastest-warming state in the United States, faces significant challenges in managing water resources under amplified hydroclimatic variability, particularly with increasing drought frequency and severity (Union of Concerned Scientists, 2016). Snowmelt-derived surface flows and groundwater withdrawals constitute the primary water sources for municipal and agricultural demands, particularly in the Rio Grande Basin. These hydrologic systems are intricately linked through complex surface-subsurface interactions that vary across spatial and temporal scales. Without integrated, predictive modeling tools, water resources managers and planners can face difficulties in quantifying the long-term impacts of warming trends, reduced snowpack, and intensified groundwater extraction on water availability.

Previous studies have addressed components of New Mexico's hydrology using standalone or loosely coupled models. Ketchum (2016) estimated groundwater recharge across the state from 2000 to 2013 using a daily soil water balance model informed by remote sensing datasets. Xu (2018) refined this approach by improving the estimation of focused recharge. However, these studies emphasized historical simulations and did not provide forward-looking projections, which are critical for long-term planning. Moreover, integrating surface and subsurface hydrology at a statewide scale remains challenging because of the complexity of coupling processes, heterogeneity in data formats, and substantial computational requirements.

Recent advancements in coupled hydrologic modeling have demonstrated the potential for integrated approaches. Jafari et al. (2021) coupled the Soil and Water Assessment Tool (SWAT) (Arnold et al., 1998) with MODFLOW, a groundwater model developed by USGS, to simulate surface-subsurface hydrologic interactions in a 1,452 km^2 watershed, identifying curve number—a dimensionless hydrological parameter developed by the USDA Natural Resources Conservation Service (NRCS)—and hydraulic conductivity as key parameters. Similarly, Sridhar et al. (2018) integrated the Variable Infiltration Capacity (VIC) model (Hamman et al., 2018), a macroscale land surface model, with MODFLOW to improve streamflow predictions in a 186,479 km^2 watershed in Idaho. Their findings underscored the value of coupled models for sustainable watershed management. However, their study was limited to a 27,972 km^2 aquifer region and a 5-year calibration period because of computational constraints. Given New

Mexico's area of approximately 314,000 km^2, a scalable, automated, and computationally efficient framework is essential for statewide hydrologic modeling. In this study, we focused on the development of a software framework for coupled surface-subsurface hydrologic modeling.

1.2. Study Goal and Contributions

The objective of this study is to develop a high-resolution, fully automated software framework that couples the VIC land surface model with the MODFLOW 6 (MF6) groundwater model for statewide application in New Mexico. The purpose of the framework is to simulate water availability under both historical and projected climate conditions, enabling more accurate assessments of drought vulnerability.

We present the following key contributions through this research:

1. A reproducible workflow that supports data preprocessing, model configuration, and execution, with support for scripting and version tracking.
2. A set of conversion tools to transition from legacy or incompatible formats (e.g., VIC Classic, MF-OWHM) to scalable, NetCDF-based or parallelization-compatible formats required for coupling (e.g., VIC Image, MF6).
3. A coupling controller VIC-MF6 that links surface and subsurface processes using the MF6 Application Programming Interface (API) based on the eXtended Model Interface (XMI), allowing exchange of hydrologic fluxes such as groundwater discharge and baseflow at each simulation stress period.
4. A statewide application of the coupled model to the Rio Grande Basin, featuring simulations over the historical period from 1940 to 2023 driven by observed meteorological data from 1990 through 2023 (1940–1989 using subsurface general head boundary conditions within MF6), and extended through 2100 using downscaled Coupled Model Intercomparison Project Phase 6 (CMIP6) (Eyring et al., 2016) climate projections, all at a spatial resolution of 1/32°.

1.3. Framework Architecture Overview

The full modeling framework developed in this study comprises four integrated software components:

1. VIC Input Generation Pipeline: A modular preprocessing system built using the Geographic Resources Analysis Support System (GRASS) (Neteler et al., 2012), shell scripts, and custom C programs, that generates all VIC input layers (soil, vegetation, meteorology, Leaf Area Index [LAI]). This pipeline supports generalized applications to any domain given appropriate source datasets.
2. VIC Classic to VIC Image Converter: A dedicated C program that translates VIC Classic text-based input files into VIC Image NetCDF input files, enabling spatially parallel simulation and flux exchange. The tool automates input parsing, domain generation, and parameter transformation.
3. The Rio Grande Transboundary Integrated Hydrologic Model (RGTIHM) to MF6 Converter: A Python-based system built using FloPy that parses the original MF-OWHM implementation of the RGTIHM and generates a functionally equivalent MF6 model. The converter preserves all MF6-compatible inputs, including stress periods, wells, grid geometries, and boundary conditions, and produces spatial verification layers in the GeoPackage format.
4. VIC-MF6 Coupling Controller: A Python module that synchronizes VIC and MF6 model execution at each time step using the XMI. This component handles state management, water balance checking, and file Input/Output (I/O) between VIC's NetCDF outputs and MF6's recharge and baseflow fields.

1.4. Broader Impact and Use Case

To demonstrate its performance and applicability, the coupled framework was deployed for surface water across the entire state of New Mexico, with a groundwater focus on the Lower Rio Grande Basin as defined by the RGTIHM. Model simulations spanned the historical period from 1940 to 2020, with future scenario support available through climate-forcing extensions until 2100. To the best of our knowledge, this study presents the first successful integration of surface and subsurface hydrologic modeling across the entire state of New Mexico (for surface water) and the Lower Rio Grande Basin (for subsurface water) using a fully coupled, open-source, and scalable simulation framework. We plan to couple the Middle Rio Grande Basin as well.

2. METHODS AND DATA

This section describes the methods and datasets used to develop the VIC-MF6 coupled hydrologic modeling framework for New Mexico. Section 2.1 reviews foundational groundwater modeling studies, including the Lower Rio Grande (LRG) RGTIHM developed by Hanson et al. (2020) and the Middle Rio Grande (MRG) Basin MODFLOW model by McAda and Barroll (2002). It describes the hydrogeologic structure, groundwater flow patterns, and key stresses such as pumping and recharge. The section also explains the conversion of the original RGTIHM from MF-OWHM to MF6 to support integration with modern modeling workflows.

Section 2.2 describes the configuration of the surface water model using VIC. It outlines the spatial domain, model resolution, and parameter downscaling methods. The section also presents the preparation of meteorological forcing data consistent with the spatial and temporal requirements of the coupled framework.

Section 2.3 presents the approach used for hydrologic forecasting under future climate conditions. It describes the use of downscaled CMIP6 projections to provide temperature, precipitation, and radiation inputs for the hydrological model, and extrapolation of some inputs for the future. These data enable long-term simulations to evaluate the potential impacts of climate variability on regional hydrology.

Section 2.4 details the architecture of the coupled modeling framework developed to automate and manage model workflows. It introduces the use of GRASS for spatial preprocessing, shell and Python scripts for automation, and C programs for raster data handling. The section also describes the implementation of the coupled VIC-MF6 simulation loop, designed to support high-resolution, long-term analysis across the study domain.

2.1. Groundwater Modeling

We adopted MF6 (Langevin et al., 2017) as the groundwater model for this study. MF6 is a modular, finite-difference groundwater flow model designed for flexible, large-scale hydrologic applications. Its object-oriented structure supports multiple groundwater flow models within a single simulation domain, enabling adaptive spatial resolution critical for New Mexico's heterogeneous aquifers. MF6's parallelization, implemented via the Message Passing Interface (MPI) (Forum, 1994), optimizes performance on High-Performance Computing (HPC)

environments, making it suitable for large-scale statewide modeling. The model supports unstructured grids, enhancing computational efficiency and accuracy in representing complex hydrogeologic conditions, such as those in the Rio Grande Basin. Sections 2.1.1–2.1.7 summarize the methods and findings of Hanson et al. (2020) for Rio Grande transboundary hydrologic modeling. Sections 2.1.8 and 2.1.9 discuss our efforts to convert the LRG and MRG models to MF6.

2.1.1. Rio Grande Transboundary Hydrology

The RGTIHM by Hanson et al. (2020) was designed to simulate the movement and use of groundwater in the Transboundary Rio Grande (TRG) region, which is considered the LRG region of the U.S. Developed using the MODFLOW One-Water Hydrologic Flow Model (MF-OWHM) version 2, it integrates surface and groundwater systems to analyze water use, availability, and movement within the active model domain. The model provides a comprehensive tool for stakeholders to evaluate surface water operations and address water use issues in the region. Originally calibrated for the period 1940–2014, the RGTIHM requires periodic updates as hydrologic conditions evolve, as new data become available. The development of the RGTIHM followed a three-phase approach:

1. Data collection and compilation,
2. Development of a hydrogeologic framework, and
3. Construction and calibration of the hydrologic model.

To refine the hydrologic representation, the model incorporates the Basin Characterization Model (BCM) to account for precipitation, recharge, and runoff during both dry and wet periods from 1940 to 2014. Key features of the RGTIHM include

- Integration of surface water and groundwater interactions,
- Estimation of tributary boundary inflows from ephemeral streams,
- Simulation of supply-constrained and demand-driven water use, and
- Automated calibration using PEST software for model refinement.

2.1.2. Spatial and Temporal Configuration of the RGTIHM

The RGTIHM covers 1,760 mi^2 with a finite-difference grid consisting of 912 rows and 328 columns (299,136 cells) across nine geologic layers, totaling 816,886 active cells. A horizontal

resolution of 10 ac per cell (201 m by 201 m) was selected to enhance accuracy in land-use and water-supply characterization. The grid is rotated 24° west of the north to align with regional geological features. The model layers correspond to five hydrogeologic units described by Sweetkind (2017) with the uppermost aquifer layer ranging from 50 ft to 110 ft thick and the deepest layer representing pre-Santa Fe Group rocks, varying between 500 ft and 607 ft in thickness. Temporally, the RGTIHM employs monthly stress periods and semi-monthly time steps, spanning 74.8 years from March 1940 to December 2014. Figures 1–3 from Hanson et al. (2020) visualize the study area in great detail.

2.1.3. Groundwater Flow and Structural Influences

Groundwater flows from upland areas toward the Rio Grande through the Santa Fe Group of aquifers, primarily moving northwest to the southeast. Structural features such as bedrock uplifts and faults influence flow patterns, creating distinct groundwater subregions. Historical data shows steep hydraulic gradients, with water moving from the Black Range and Caballo Mountains toward the Rincon Valley and Mesilla Basin.

2.1.4. Effects of Pumping and Recharge Sources

Since the 1950s, increased pumping has disrupted natural groundwater flow, leading to regional cones of depression, particularly in the Mesilla Basin. Seasonal declines in groundwater levels are linked to agricultural, municipal, and industrial withdrawals. Groundwater recharge sources include precipitation, streamflow, irrigation, and subsurface inflows, while outflows occur through pumping, evapotranspiration, and baseflow into streams. The El Paso Narrows act as a barrier, limiting groundwater movement from the Mesilla Basin into the Hueco Bolson. The main recharge source, apart from precipitation, is the surface water from the Rio Grande and its tributaries. This water resource is expressed as a surface water network in the SFR2 package in the MF-OWHM, which contains 566 segments, represented by 9,774 reaches, 61 diversions, 98 inflows, and 3 outflows.

2.1.5. Groundwater Use Trends

Groundwater irrigation in the TRG region expanded rapidly from the 1950s because of drought, with the number of wells increasing from 11 in 1946 to over 1,000 by 1957. Currently, there are around 3,744 irrigation wells in New Mexico and 215 in Texas, though their operational

status is uncertain. The RGTIHM includes a total of 14,698 wells, categorized into agriculture (3,959 wells), municipal and industrial (1,874 wells), and domestic (8,865 wells). Agricultural groundwater withdrawals have fluctuated with climate conditions, peaking during droughts. In Doña Ana County, usage dropped from 73,000 ac-ft in 1975 to about 57,000–58,000 ac-ft in the wet 1980s, but surged to 95,000 ac-ft in the early 2000s. Withdrawals in the LRG district doubled from 140,000 ac-ft in 2010 to 280,000 ac-ft in 2011, highlighting increasing reliance on groundwater.

2.1.6. Groundwater Pumping

Municipal and industrial groundwater pumping in the TRG region has increased since the 1940s, peaking in New Mexico at 64,000 ac-ft in 2009 because of population growth. In Texas, pumpage peaked at 28,000 ac-ft around 2000, while municipal pumping in Mexico began in 2010 and continues to rise. Major users include Las Cruces, El Paso, and the Camino Real Regional Utility Authority. Several smaller utilities also contribute, with 1,414 wells in New Mexico, 427 in Texas, and 33 in Chihuahua, Mexico. These trends can be observed in Figures 4 and 5 from Hanson et al. (2020).

2.1.7. Domestic and Small-Scale Groundwater Use

Domestic well pumpage in Doña Ana County decreased from approximately 2,300 ac-ft in 1990 to 650 ac-ft in 2010, based on estimates compiled by the New Mexico Office of the State Engineer (NMOSE). The NMOSE reported 8,817 domestic wells in the New Mexico portion of the TRG region, but detailed information on active wells was scarce, making it difficult to determine the exact number of active wells. The Texas Water Development Board (TWDB) reported 60 domestic wells in the Texas part of the region. Similarly, the exact number of active wells was unclear. The RGTIHM plays a crucial role in advancing the understanding of groundwater dynamics in the Rio Grande Basin, facilitating better decision-making for water resources management in the transboundary region.

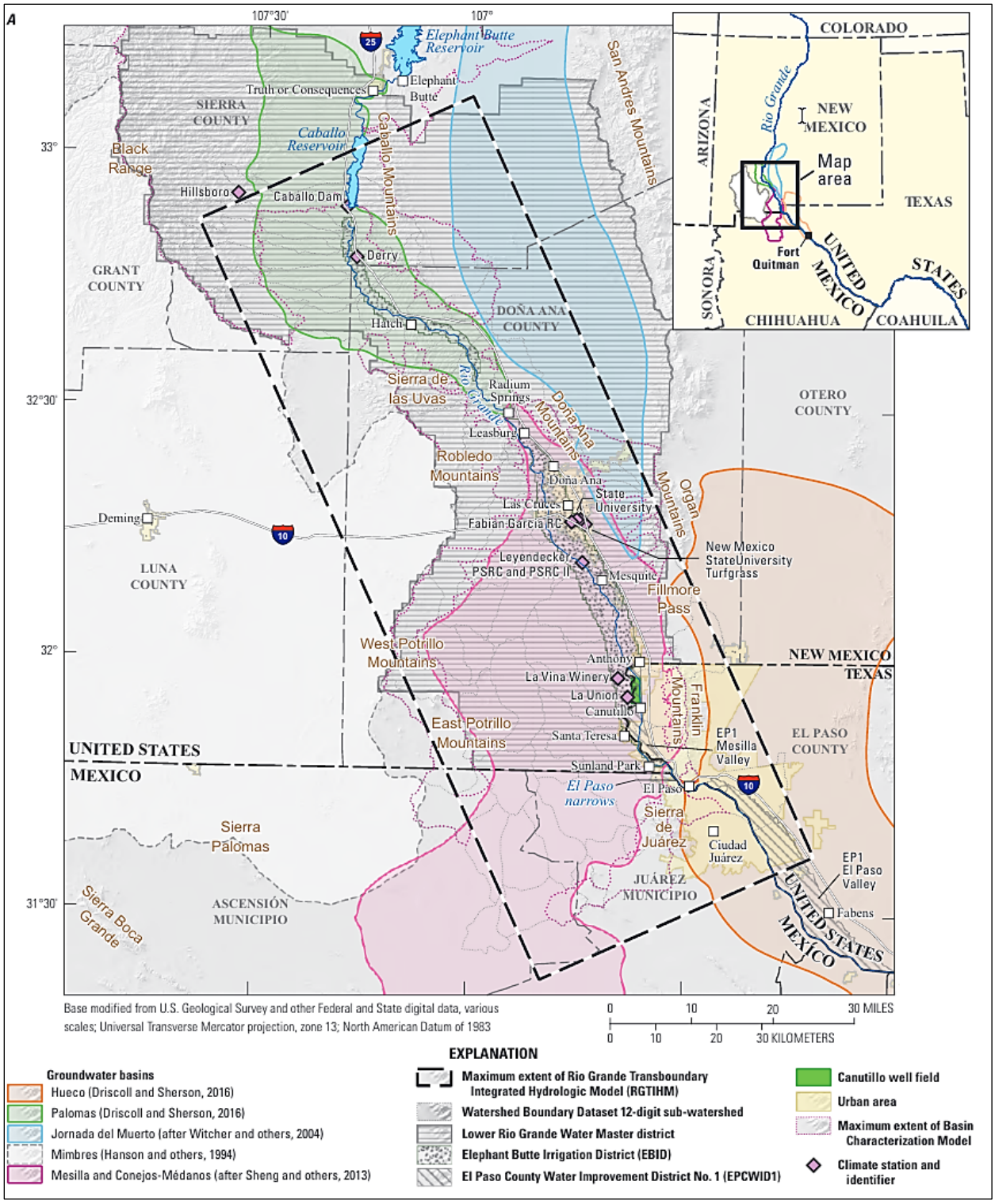

Figure 1. Total Extent of the RGTIHM's Modeling Area Including Watersheds and Groundwater Basins. Figure 1A from Hanson et al. (2020).

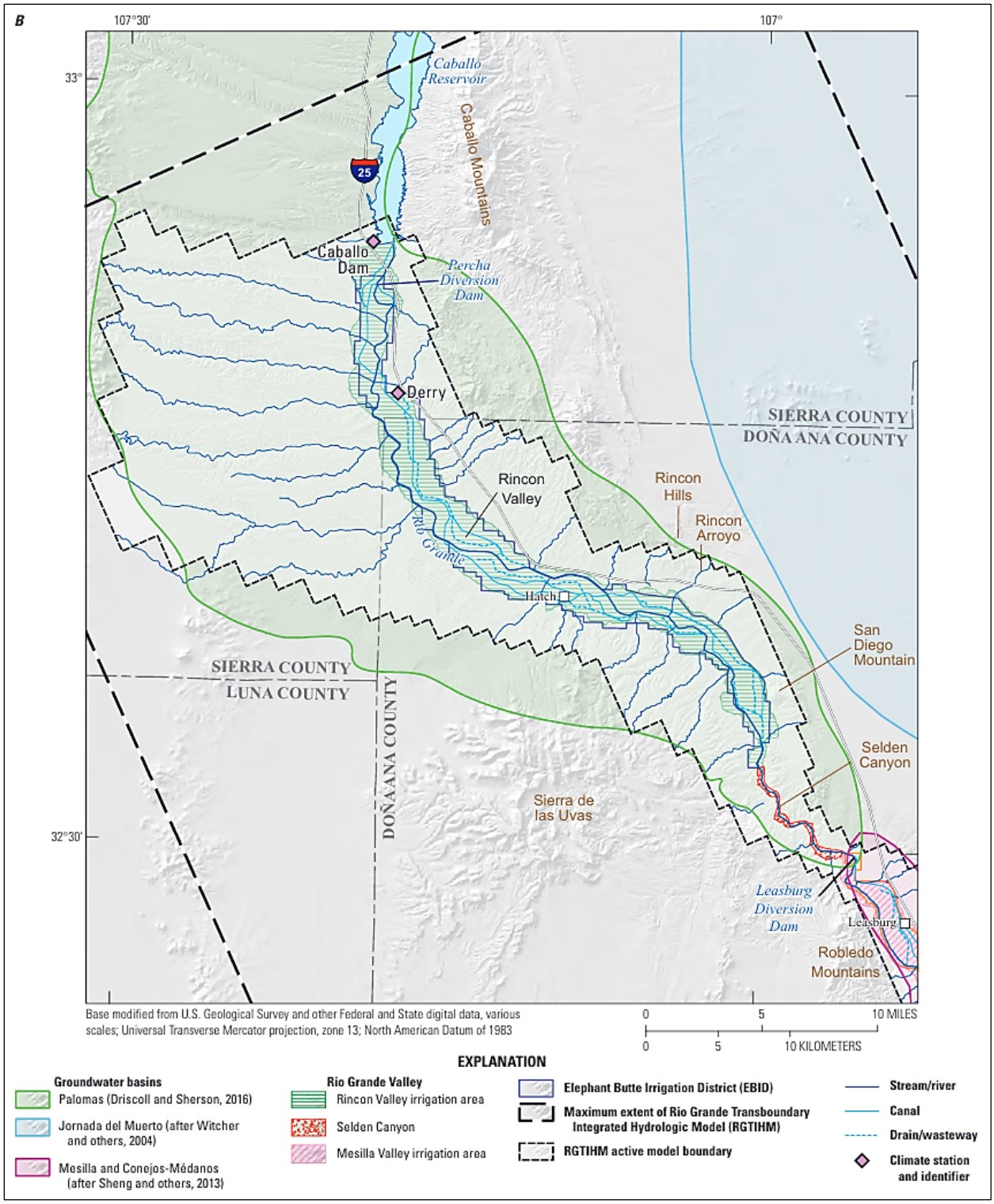

Figure 2. The Rincon Valley Basin. Figure 1B from Hanson et al. (2020).

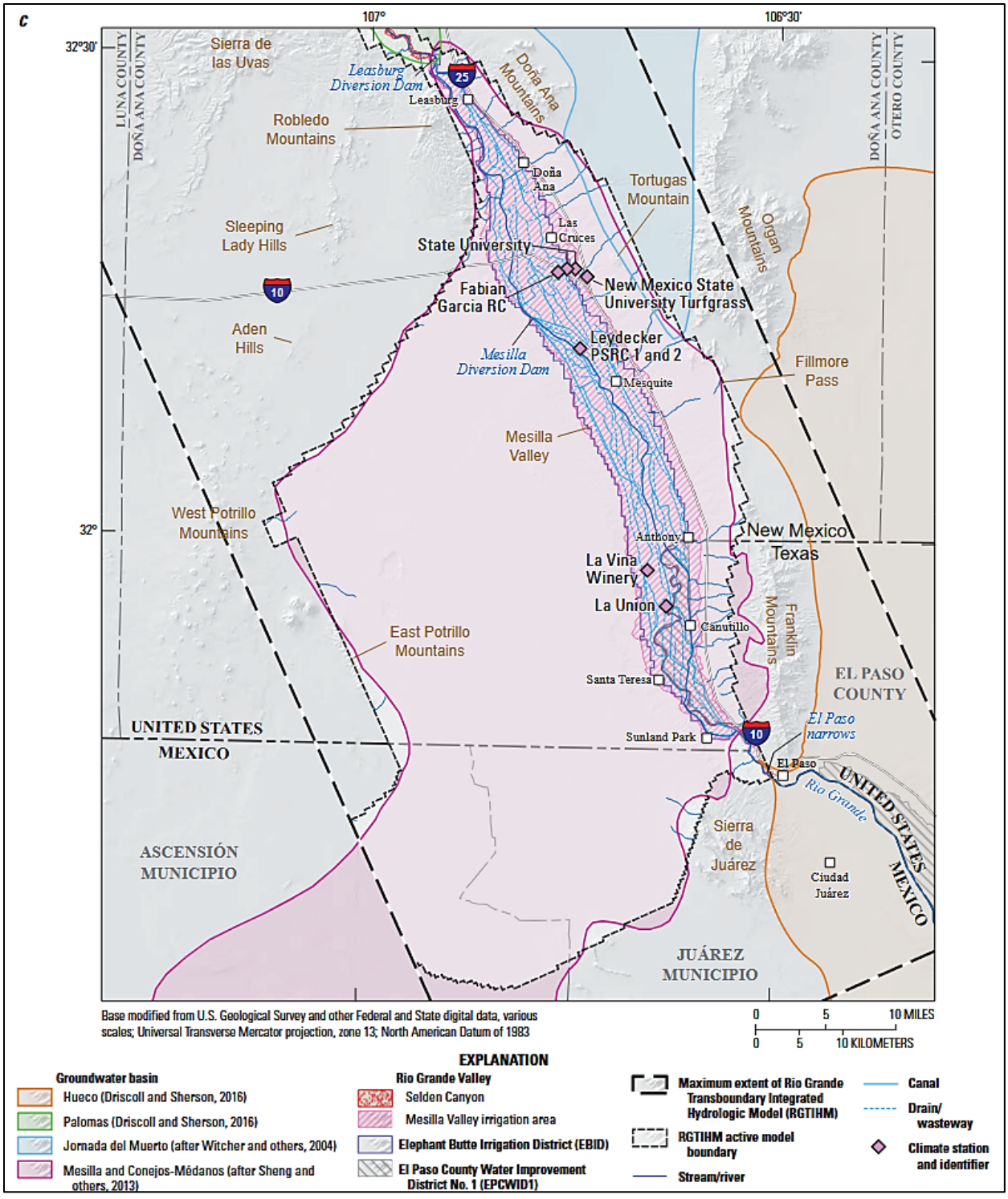

Figure 3. The Conejos-Medanos Basin. Figure 1C from Hanson et al. (2020).

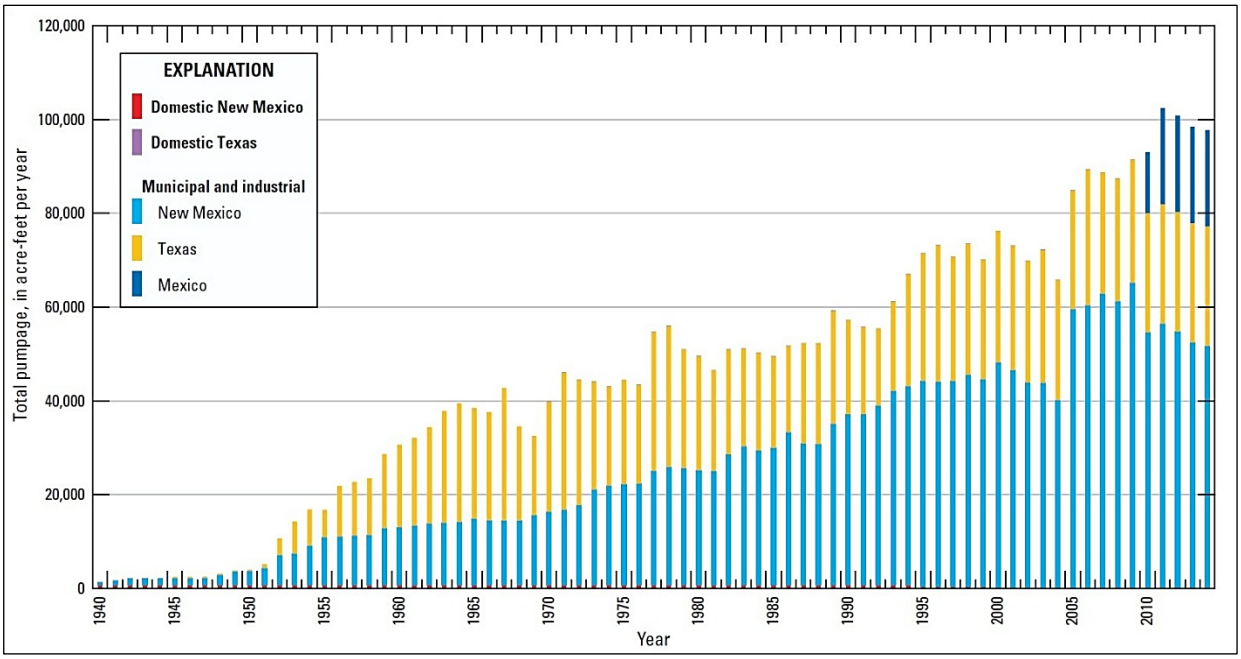

Figure 5. Estimated Groundwater Pumpage in the Transboundary Rio Grande, Municipal and Industrial, and from Domestic Wells. Figure 11B from Hanson et al. (2020).

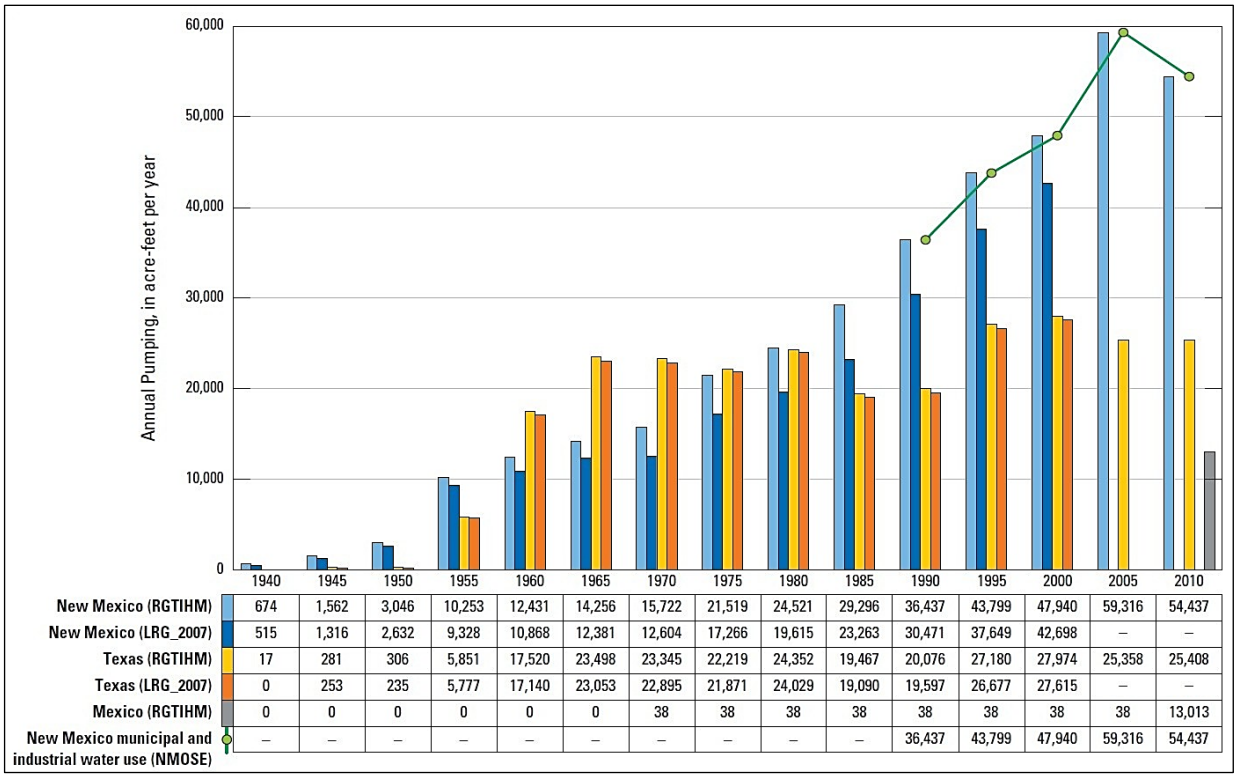

	1940	1945	1950	1955	1960	1965	1970	1975	1980	1985	1990	1995	2000	2005	2010
New Mexico (RGTIHM)	674	1,562	3,046	10,253	12,431	14,256	15,722	21,519	24,521	29,296	36,437	43,799	47,940	59,316	54,437
New Mexico (LRG_2007)	515	1,316	2,632	9,328	10,868	12,381	12,604	17,266	19,615	23,263	30,471	37,649	42,698	–	–
Texas (RGTIHM)	17	281	306	5,851	17,520	23,498	23,345	22,219	24,352	19,467	20,076	27,180	27,974	25,358	25,408
Texas (LRG_2007)	0	253	235	5,777	17,140	23,053	22,895	21,871	24,029	19,090	19,597	26,677	27,615	–	–
Mexico (RGTIHM)	0	0	0	0	0	0	38	38	38	38	38	38	38	38	13,013
New Mexico municipal and industrial water use (NMOSE)	–	–	–	–	–	–	–	–	–	–	36,437	43,799	47,940	59,316	54,437

Figure 4. Estimated Groundwater Pumpage in the Transboundary Rio Grande, New Mexico, Texas, and Mexico, from the New Mexico Office of the State Engineer (NMOSE), Reported Municipal and Industrial Pumpage. Figure 11A from Hanson et al. (2020).

2.1.8. Conversion of the RGTIHM from the MF-OWHM to MF6

To leverage the RGTIHM's calibrated parameters, we converted its MF-OWHM implementation to MF6 for the 1940–2014 period. The conversion using the FloPy Python package (explained in Section 2.4) preserved the RGTIHM's grid geometry (201 m by 201 m), stress periods, well configurations, and boundary conditions, including recharge and flow barriers.

2.1.9. Middle Rio Grande Basin Hydrology

McAda and Barroll (2002) developed a MODFLOW-2000 (MF2K) model for the MRG Basin, spanning Cochiti to San Acacia, New Mexico, to study the Santa Fe Group aquifer system, which includes middle Tertiary to Quaternary formations and post-Santa Fe Group valley-fill deposits, amid concerns over water availability due to significant groundwater declines since the 1940s driven by population growth and increased extraction. The model, aimed at enhancing water resources management by integrating surface water and groundwater interactions, features nine layers from the water table to the pre-Santa Fe Group basement (up to 9,000 ft below NGVD 29), with a horizontal grid of 156 rows and 80 columns at 1 km cell spacing, simulating pre-development steady-state and transient conditions from 1900 to March 2000, including seasonal variations post-1990 for better trend accuracy. It incorporates boundary conditions including mountain-front recharge, tributary inflows, subsurface contributions, and seepage from irrigation canals, agricultural fields, and septic systems, alongside groundwater withdrawals as specified flow boundaries and surface water interactions (e.g., Rio Grande, Jemez River, Cochiti Lake) as head-dependent flow boundaries, while hydraulic properties are parameterized with horizontal hydraulic conductivity ranging from 0.05 ft to 60 ft per day, a vertical anisotropy ratio of 150:1, specific storage at 2×10^{-6} per ft, specific yield at 0.2, and variable horizontal anisotropy reflecting north-south fault orientations for accurate subsurface flow representation.

To leverage the advantages of MF6, we first converted the MF2K model to MODFLOW-2005 (MF5) using the MF2KtoMF5 converter and then converted the MF5 model to MF6 using the MF5to6 converter. The model was divided into six submodels using the FloPy Python package, allowing for performance comparisons between sequential and parallel configurations. The MF6 equivalents of the MF-OWHM packages used in our model are documented separately.

We dropped the MRG Basin Model from this study for now because of the software issue reported in Section 4.1.3.

2.2. Surface Water Modeling

We used the VIC version 5 model to simulate surface water for this study. VIC is a grid-based, semi-distributed hydrologic model that is well-suited for large-scale, high-resolution surface water resource simulations. VIC provides physically based representations of key hydrologic processes, including evapotranspiration, soil moisture storage, baseflow generation, and snowpack dynamics, which is particularly critical for hydrologic modeling in New Mexico's mountainous regions. The model's ability to explicitly represent energy balance and snow accumulation/melt processes makes it ideal for snow-fed river systems in arid and semi-arid regions. VIC operates on a spatially distributed grid, allowing high-resolution simulations where each grid cell functions as an independent hydrologic unit while maintaining lateral water movement controls.

The model is fully parallelized utilizing the MPI, enabling scalable simulations on HPC environments to efficiently process long-term climate and hydrology datasets over large domains. VIC has been widely used in land surface hydrology studies, climate impact assessments, and operational forecasting systems (Hamman et al., 2018; Liang et al., 1994; Maurer et al., 2002).

2.2.1. Model Configuration and Spatial Resolution

We developed a physically based, high-resolution hydrologic model tailored specifically for the state of New Mexico using the VIC model. The motivation behind this effort is to improve our ability to simulate key water balance components, including evapotranspiration, soil moisture, and runoff across different hydroclimatic regions of New Mexico. Given the diverse physiographic and climatic conditions of the state, a distributed hydrologic model like VIC allows for a more detailed representation of hydrologic processes compared to lumped or conceptual models. This model serves as a critical tool for water resources management, climate impact assessment, and hydrologic forecasting.

The base parameterization was derived from a validated VIC calibration at a 1/8° resolution (Yang et al., 2019). To enhance spatial details, we downscaled soil and vegetation parameters to

1/32° (~3.375 km), aligning with the coupled framework's requirements while preserving calibration integrity. The new MF6 model retains the RGTIHM's 201 m-by-201 m grid, with data exchange facilitated by a joint database described in Section 2.4.6.2.

The VIC model operates on a daily time step, resolving water and energy balances to capture seasonal and interannual variability. Soil properties, including texture and depth, were sourced from a 2016 high-resolution dataset (Ketchum, 2016). Vegetation parameters, derived from satellite-based land cover, reflect evapotranspiration regimes across ecological zones. The coupled framework VIC-MF6 integrates VIC (1990–2020 historical, 2020–2100 projected) and MF6 (1940–2014 historical, 2015–2100 extrapolated), enabling simulations from 1940 to 2100. The name VIC-MF6 emphasizes the role of MF6 as the primary driver in the coupling interface, enabling integration that is not possible with its previous versions.

2.2.2. Parameter Downscaling

Since we adopted a previously validated VIC calibration as our base model, the challenge was to downscale the soil and vegetation parameters from the original resolution of 1/8° to 1/32° while preserving the integrity of the calibration. The VIC model requires detailed soil and vegetation parameter datasets, including 53 soil-related parameters distributed across three soil layers and vegetation inputs such as the vegetation library and the Leaf Area Index (LAI).

To achieve the desired resolution, we tested multiple interpolation methods using GRASS, which is a powerful computational engine for raster, vector, and geospatial processing (Neteler et al., 2012). Nine interpolation methods were considered, with trials performed to assess their effectiveness. After evaluating the results, we selected v.surf.rst as the preferred interpolation method for downscaling. This method provided the most stable and spatially consistent results, ensuring a smooth transition between spatial scales without introducing artifacts. The downscaling process was conducted using GRASS and shell scripting, automating the resampling workflow for all parameters. The interpolation process included the following steps:

1. Set the computational region to align with the target grid resolution.
2. Perform interpolation of soil parameters using v.surf.rst.
3. Extract interpolated raster values at grid cell centers.
4. Generate and export the finalized raster dataset.

Through this process, we successfully downscaled the soil and vegetation parameter datasets while preserving the original VIC calibration integrity. This refinement enhances the model's ability to resolve local-scale hydrologic processes while maintaining the reliability of the base parameterization. We note that the downscaled parameters represent spatially refined initial estimates rather than recalibrated values. Consistent with the scope of this study, which focuses on developing the coupling framework, further calibration at finer resolution is deferred to future work to ensure physical consistency and optimal model performance. In addition, a systematic comparison of parameter transfer approaches, including direct mapping and spatial interpolation, is also identified as an important direction for future work.

2.2.3. Meteorological Forcing Data

For this study, we compiled a high-resolution, long-term meteorological forcing dataset spanning from 1991 to 2023 at a daily time step. The data sources and preprocessing steps are as follows:

1. Precipitation was derived from the Parameter-elevation Regressions on Independent Slopes Model (PRISM) Climate Group dataset (PRISM Group, 2014), ensuring high accuracy in spatial and temporal variability.
2. Minimum and maximum temperatures were also sourced from the PRISM, providing continuous and quality-controlled temperature fields.
3. Shortwave and longwave radiation were not directly available, so they were estimated using the Mountain Microclimate Simulation Model (MTCLIM) (Hungerford et al., 1989)—a widely used radiation estimation approach in land surface modeling.
4. Wind speed was obtained from the Gridded Surface Meteorological (gridMET) dataset (Abatzoglou, 2013), which offers high-resolution, gridded wind speed data suitable for VIC applications.
5. Vapor pressure was required by the VIC model as part of the meteorological forcings and added by the MTCLIM.
6. Surface pressure was calculated using the standard atmospheric pressure equation from the US Standard Atmosphere (NOAA, 1976) incorporating elevation-dependent adjustments for improved accuracy.

The equation for the surface pressure is defined as:

$$P = P_b \left(1 - \frac{L_b h}{T_b}\right)^{\frac{g_o M_o}{R L_b}} \quad (1)$$

where h is the elevation (m), P is the pressure (hPa) at elevation h, P_b is the reference pressure at sea level (1013.25 hPa), L_b is the lapse rate (6°C/km), T_b is the base temperature (K), g_0 is the standard gravitational acceleration (9.81 m/s^2), M_0 is the molar mass of Earth's air (0.029 kg/mol), and R is the universal gas constant (8.31 J/mol/K).

All meteorological forcings were originally at a 4-km resolution and were spatially processed using GRASS and shell scripting to ensure alignment with our VIC grid resolution of 3.375 km (projected resolution of 1/32°). We applied a weighted averaging approach to resample and adjust these datasets to our VIC model domain, ensuring that the atmospheric forcings accurately corresponded to the hydrologic grid. The final preprocessed meteorological data were then read into Esri's Shapefile format and reformatted into VIC-compatible input files.

This rigorous data preprocessing workflow ensures that our VIC model has high-quality forcing inputs, enabling reliable simulation of hydrologic processes across New Mexico. By leveraging advanced geospatial tools and scripting automation, we efficiently handled large datasets and ensured methodological consistency in meteorological data preparation.

2.3. Projected Climate Modeling

To assess future water availability under dynamic climate conditions, we used data from the CMIP6. We explored multiple datasets from different modeling centers, ensemble members, and downscaling approaches. After comparative evaluation, we selected the MPI-ESM1.2-HR model developed by Gutjahr et al. (2019). This model provides high-resolution outputs with improved representation of atmospheric and oceanic processes, making it well-suited for hydrologic impact analysis over complex terrains such as New Mexico.

We adopted the Shared Socio-economic Pathways (SSP) SSP5-8.5 scenario, a high-emissions pathway that represents a fossil-fueled development trajectory with limited climate mitigation. This scenario was chosen to capture the upper bound of climate-driven hydrologic stress and assess system vulnerability under extreme warming conditions. Daily climate variables including precipitation, minimum and maximum temperatures, wind speed, shortwave radiation,

and longwave radiation were extracted from the MPI-ESM1.2-HR output and processed for the period extending through 2100.

To integrate the CMIP6 projections with our VIC model domain, we developed a preprocessing workflow in GRASS that includes spatial extraction and temporal formatting. The raw climate outputs were restructured into VIC-compatible meteorological forcing files. This conversion was completed for the entire simulation period, and the future forcing datasets were fully integrated with the VIC model. The resulting dataset enables physically based simulations of long-term water balance trends and climate-driven hydrologic shifts across New Mexico.

The RGTIHM MF6 model was also extended through 2100 by applying a constant future pumping rate equal to the historical median increased by 10%, based on projected regional population growth (capped at 7% and rounded to the nearest tenth), resulting in a total simulation period spanning 1940 to 2100 (161 years).

2.4. Framework Architecture

2.4.1. Modular Design for Hydrologic Modeling

To address the complexity of statewide hydrologic modeling and ensure reproducibility, we designed a modular framework architecture that integrates geospatial preprocessing, parameter handling, model configuration, simulation execution, and postprocessing into a streamlined computational pipeline. The architecture supports automation at every stage of the VIC and MF6 modeling processes, aiming to minimize manual intervention while maximizing efficiency and transparency. Built entirely on open-source technologies including GRASS, Portable Operating System Interface (IEEE, 2024) (POSIX)-compliant Bash scripts, and C programs, the framework ensures flexibility, accessibility, and interoperability for researchers and practitioners. This modular approach breaks down the modeling process into distinct, interlinked stages, each with a specific functional role, allowing for seamless data flow and consistent execution across large spatial domains and extended temporal periods.

2.4.2. GRASS-Based Spatial Preprocessing

At the heart of the framework lies a robust geospatial preprocessing stage, powered by GRASS as the core engine for spatial data management and transformation. This stage focuses on handling diverse datasets such as land cover, soil properties, vegetation characteristics, and

meteorological grids, ensuring they are spatially aligned and formatted for hydrologic modeling. GRASS facilitates critical operations such as raster-vector conversion to harmonize data types, geospatial masking to isolate areas of interest, and spatial interpolation to refine coarse datasets to finer resolutions. For example, interpolation techniques such as v.surf.rst are used to downscale soil and vegetation parameters, ensuring compatibility with VIC's resolution requirements and alignment with MF6 grid cells. The GRASS environment also serves as the spatial backbone, setting consistent gridded computational region boundaries and extracting hydrologic attributes such as soil moisture capacity and runoff potential. All spatial operations are conducted within project-specific GRASS projects and mapsets (GRASS' terminology for map sets), providing an organized structure for managing data layers and ensuring reproducibility of geospatial workflows across different modeling scenarios.

2.4.3. Workflow Pipeline with Shell Scripting and C Programs

The orchestration of the modeling pipeline is achieved through a suite of modular, POSIX-compliant Bash scripts that automate and sequence the workflow across preprocessing, simulation, and output analysis stages. These scripts act as the glue between different components, managing the execution of GRASS operations, organizing file systems, setting environment variables for computing processes, and coordinating the order in which VIC and MF6 simulations are performed. The scripting layer ensures that each modeling step—ranging from input file preparation and time-step-specific execution to organized output management—is performed reproducibly and without manual intervention. This automation not only reduces the risk of human errors, but also simplifies debugging, supports batch processing, and enables scalability to large spatial domains and multi-decadal temporal windows. By providing a structured approach to workflow management, the scripts create a seamless and efficient environment that can handle the computational demands of statewide hydrologic modeling.

To bridge the gap between geospatial preprocessing and model simulation, we developed a set of C programs optimized for speed and memory efficiency. These programs focus on translating the processed outputs from GRASS into VIC-compatible formats, ensuring that the spatially refined data is preserved and correctly structured for simulation. Specifically, the C programs convert text-based interpolated values into binary VIC parameter files, including datasets for soil properties, vegetation characteristics, and time series data. Given VIC's strict

requirements for file formats and efficient I/O handling, the use of compiled C programs significantly reduces the time required for preprocessing large-scale datasets, making the framework suitable for HPC environments. This translation layer ensures that the geospatial data is seamlessly integrated with the VIC simulation engine, maintaining data integrity and computational efficiency throughout the modeling process.

2.4.4. VIC Classic to Image Driver Migration

VIC supports two different model configurations: (1) Classic based on text input files and (2) Image based on NetCDF input files. Each model configuration is simulated or "driven" by its corresponding VIC driver. Our model was initially downscaled from the Contiguous United States (CONUS) VIC Classic model by Yang et al. (2019), which follows the time-over-space approach. In this approach, the model simulates all the time steps for a single cell before moving to the next cell. This sequential processing makes the VIC Classic Driver unsuitable for coupled modeling applications, where time-wise synchronicity between surface and groundwater processes is important. Coupled modeling requires the space-over-time approach, which processes all grid cells for a single time step before advancing to the next time step. The VIC Image Driver supports the space-over-time approach, making it essential for dynamic coupling with MF6. This limitation of the VIC Classic Driver necessitated migration to the VIC Image Driver, which features a fundamentally different HDF5-based structure compared to the text-based VIC Classic Driver.

2.4.5. MF-OWHM to MF6 Conversion

To extend the framework's capability to groundwater modeling while ensuring a reproducible foundation for the subsequent coupling with VIC, we implemented a Python-based conversion of the RGTIHM from its original MF-OWHM implementation to MF6. This standalone conversion was essential, as the coupling framework relies on a consistent and reproducible MF6 model to integrate groundwater dynamics with VIC's surface water processes effectively. Leveraging the FloPy package for model construction and management, the conversion process was designed to preserve the hydrologic integrity of the original model without altering any input data, ensuring fidelity to the source while adapting to MF6's modern architecture, which offers improved numerical stability and flexibility. The method involved initializing a new MF6 simulation with a designated workspace and model name, followed by

configuring key packages such as Temporal Discretization (TDIS), Structured Discretization (DIS), Output Control (OC), Iterative Model Solution (IMS), Initial Conditions (IC), and Well (WEL). A sample cross section of the model is illustrated in Figure 6. The Python script utilized additional libraries, including NumPy for array operations, Matplotlib for diagnostic plotting, and GeoPandas for grid export to GeoPackage formats. The DIS package adaptation addressed key differences between MF-OWHM and MF6, including flipping the grid orientation from top-down to bottom-up using np.flipud, converting coordinate origins from upper-left to lower-left, and importing elevation data from text files. Parallel processing using Python's multiprocessing module (with cpu_count) was employed to enhance performance during data processing, while modules rasterio and contextily supported spatial data handling and basemap integration for visualization. This Python-driven approach ensured a systematic and reproducible translation, laying the groundwork for seamless integration of groundwater dynamics with surface water processes modeled by VIC.

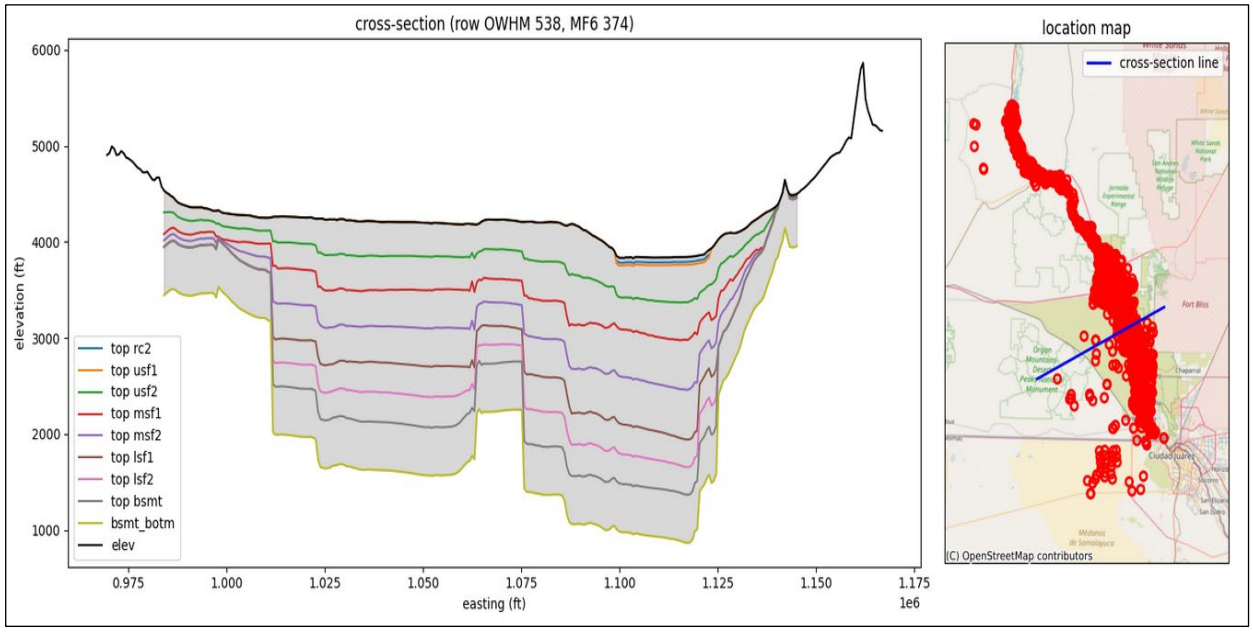

Figure 6. Sample Cross Section of the RGTIHM MF6 Model.

2.4.6. Coupled Simulation Framework

The coupled simulation framework VIC-MF6 integrates the VIC model with MF6 to simulate the dynamic interplay between surface water and groundwater systems, emphasizing the exchange of key hydrologic fluxes across the land surface-groundwater interface. The hydrologic

method centers on the Unsaturated Zone Flow (UZF) package within MF6, which facilitates the bidirectional transfer of water. VIC generates baseflow (OUT_BASEFLOW), representing the infiltration from surface processes, which is translated into infiltration (finf) for MF6's UZF package. This flux is adjusted using area-weighted ratios to account for differences in spatial resolution between the models. In return, MF6 calculates groundwater discharge to the land surface (gwd) via the UZF package, which influences VIC's soil moisture dynamics. The gwd is incorporated into VIC's initial moisture (init_moist) parameter for the third soil layer when positive, reflecting groundwater contributions to surface conditions; if gwd is zero, init_moist is set to a minimal value to maintain stability. This approach ensures a physically consistent representation of water movement, capturing feedback mechanisms critical for simulating integrated hydrologic processes over extended temporal scales, such as the 161-year period from 1940 to 2100. The coupling region of VIC and MF6 is where hydrologic exchange is supposed to happen.

2.4.6.1. Hydrological Exchange. The exchange loop, managed by the CouplingManager class, orchestrates the monthly coupling between VIC and MF6, aligning their simulations to reflect integrated hydrologic dynamics. The process begins with VIC and MF6 running a monthly stress period, producing three key outputs: two from VIC—a state file for pausing and resuming the surface simulation and a water balance (wbal) file containing OUT_BASEFLOW—and one from MF6, the UZF package's groundwater discharge (gwd). If gwd exceeds zero, it is area-weighted for VIC grid cells and used to update VIC's init_moist parameter in the parameter file (nc5_params.nc) for the next iteration. Otherwise, init_moist is set to zero and the wbal file is read using the netCDF4 library to extract the baseflow data, which is then converted into finf for MF6's UZF package. The finf variable is computed by weighting the baseflow with area ratios derived from the coupling table, ensuring resolution differences are addressed. Both VIC and MF6 then simulate the same monthly period and repeat the same iteration until the end of the coupling period. This loop iterates monthly, with each cycle logging the exchanged fluxes (finf, gwd) and updated init_moist values to a Comma-Separated Values (CSV) file, ensuring traceability. The coupled simulation begins on January 1, 1990, corresponding to the start of the VIC forcing dataset. Prior to this date, MF6 is run independently from its initialization date (March 1, 1940) to December 31, 1989, without requiring meteorological forcing, to establish initial groundwater conditions before coupling with VIC.

2.4.6.2. Spatial Connectivity for the Exchange. The spatial exchange is supported by a joint table generated through a shell script leveraging GRASS, which creates a coupling database matching the VIC and MF6 UZF region cells. This script intersects the VIC and MF6 cell layers to identify overlapping areas, and computes intersection areas and area ratios. VIC cells are assigned integer IDs (vic_id), while MF6 cells use a six-digit padded string format (mf6_id) based on row and column indices. The resulting mf6_vic_join table includes columns for vic_id, mf6_id, a unique coupling ID (cpl_id), intersection area (area_m2), and area ratios (mf6_area_ratio and vic_area_ratio), with the last two columns calculated as the intersection area divided by the MF6 cell area and VIC cell area, respectively. This table is exported as a CSV file with the six columns (vic_id, mf6_id, cpl_id, area_m2, vic_area_ratio, and mf6_area_ratio), providing a weighted average mechanism to exchange variables such as baseflow and gwd across differing resolutions, ensuring accurate flux distribution during the coupling process.

2.4.6.3. Implementation with the MF6 API. The MF6 API, foundational to this framework, is built upon the Basic Model Interface (BMI) standard (Hutton et al., 2020), extended by the XMI, as outlined by Hughes et al. (2022):

> "To facilitate coupling with other models, including those written in different languages, an Application Programming Interface (API) was developed for MODFLOW, leveraging the BMI standard established by the Community Surface Dynamics Modeling System (CSDMS) to provide a component-based interface for Earth-science models. This choice was informed by other coupling standards such as the Common Component Architecture, the Earth System Modeling Framework, and the Open Modeling Interface, with BMI selected for its specific design for Earth-science applications and its clear applicability to coupling MODFLOW with community-relevant process models."

Our coupling framework's highly modularized structure utilizes custom classes and functions, with the mf6.Model class initializing the model via xmipy.XmiWrapper to access the MF6 API, parsing grid and time discretization data (nlay, nrow, ncol, nper, and nstp) through XMI methods, and managing UZF variables (find and gwd) for data exchange. The VICModel class handles VIC execution, updating the global parameter file dynamically with shutil and subprocess calls, and processing NetCDF outputs with the netCDF4 library. The

CouplingManager class serves as the orchestrator, utilizing the pandas package to manage the coupling table and the NumPy package to perform array operations, implementing the exchange logic with weighted averaging based on the joint table. Figure 7 provides an overview of the coupling flowchart implemented in the framework.

The framework's modularity allows independent testing and scaling, with error handling and logging via the logging module ensuring robustness. This design, grounded in the XMI-based MF6 API, facilitates HPC compatibility and seamless integration of VIC and MF6, supporting the framework's scalability for statewide hydrologic modeling.

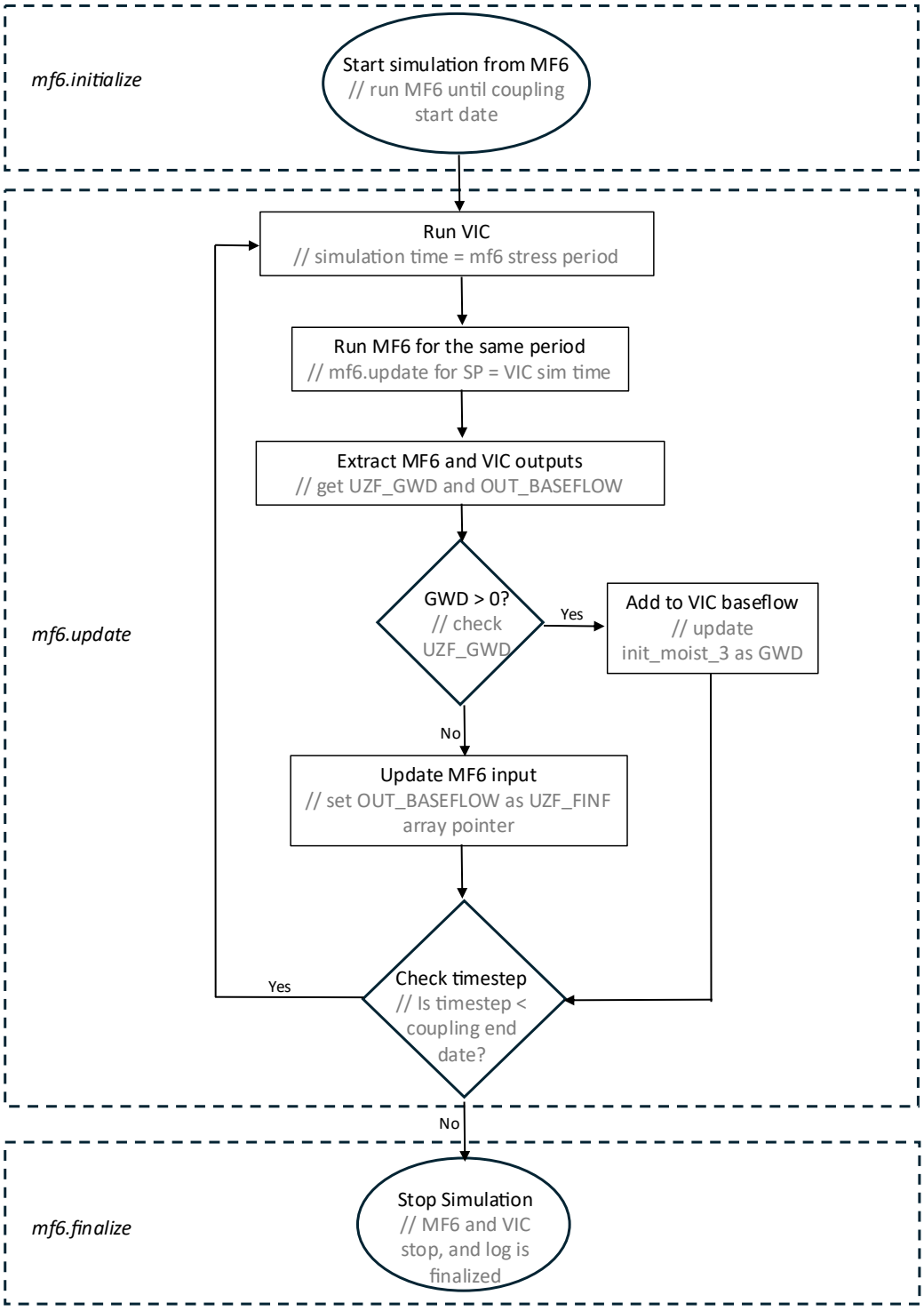

Figure 7. Flowchart of the VIC-MF6 Coupling Framework Using the MF6 API's mf6 Routines (mf6-driven control).

3. RESULTS AND DISCUSSION

3.1. VIC Classic to Image Program

The transition to VIC Image was successfully achieved across the statewide model using the VIC Classic to Image Converter, a standalone C-based tool developed to streamline VIC model transitions. This converter accepts a VIC Classic global parameter file as its sole argument and transforms the entire model—including meteorological forcing, soil and vegetation parameters, and vegetation library—into the HDF5 NetCDF format required by the VIC Image Driver. For the statewide model, encompassing diverse spatial domains, the converter completed the transformation in under 200 s, showcasing its efficiency and scalability for large-scale applications. Validation checks confirmed that the converted VIC Image Driver model preserved data integrity, with input parameters (e.g., soil properties and meteorological forcing) exhibiting zero discrepancies compared to the original VIC Classic inputs. This conversion enabled synchronized, space-over-time simulations across all grid cells per time step, fully aligning with MF6's temporal requirements. By eliminating VIC Classic's synchronicity limitations and bypassing RVIC's (an R package for running VIC Classic in parallel) memory constraints discussed in Section 3.3.1, the VIC Classic to Image Converter established a scalable and efficient surface water modeling framework, significantly enhancing the performance and compatibility of the coupled VIC-MF6 system.

3.2. MF-OWHM to MF6 Conversion

The conversion of the RGTIHM from MF-OWHM to MF6 was validated across the LRG region, and comparative runs of both models revealed no discrepancies in hydraulic inputs, confirming that the model structure—including hydraulic properties and grid configurations—was preserved during the transition as shown in Figure 8. The MF6 model maintained the original domain of 912 rows and 328 columns, with active cell counts ranging from 17,879 in Layer 1 to 112,576 in Layer 9 out of 299,136 total cells, and initial head values spanning 950 ft to 5,476 ft, aligning precisely with MF-OWHM inputs. Diagnostic visualizations, including cross sections and top elevation contours, further validated correct grid orientation and layer alignment, with inactive cell distributions matching expected geological features, establishing a reliable foundation for coupled modeling. The conversion and writing the files in MF6 format takes about 50 min.

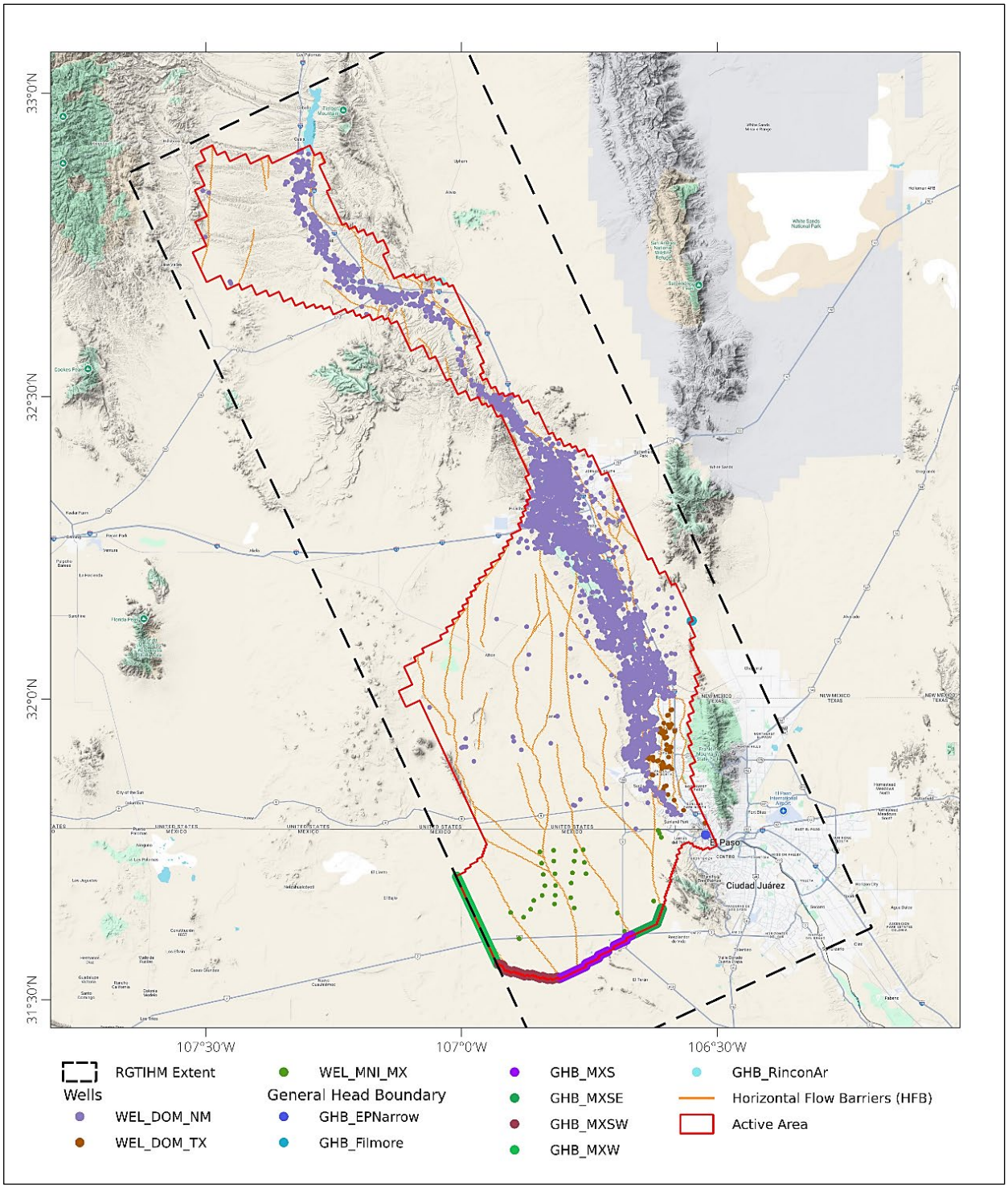

Figure 8. RGTIHM MF6 with General Head Boundary, Wells, and Horizontal Flow Barrier Packages.

3.3. Coupled Surface and Groundwater Framework

The coupled hydrologic modeling framework successfully integrated the VIC model for surface water processes with the MF6 model for groundwater dynamics, enabling bidirectional interactions between surface and subsurface hydrologic components across New Mexico's statewide hydrologic system. This integration provides a comprehensive representation of the state's water resources over a multi-decadal period from 1990 to 2100. The implementation was executed using the Python coupling framework and its outputs were postprocessed and visualized using the R programming language. Below, we discuss the performance of parallel execution, the individual VIC and MF6 results, and the framework's application for drought assessment. The run took about 650 min (almost 11 h) to complete on a single core.

3.3.1. Performance of Parallel VIC and MF6

Parallel execution of both VIC and MF6 models delivered significant performance improvements while preserving simulation accuracy across the LRG and MRG Basins. Table 1 summarizes the runtime and efficiency gains for both models under sequential and parallel configurations.

Table 1. Parallel Performance of VIC and MF6. The number of processes is given by np. Speedup is calculated by dividing the sequential runtime by the parallel runtime.

Model	Runtime (Sequential)	Runtime (Parallel)	Speedup
MF6	110 min	45 min	2.4 (n=6)
VIC Classic	69 min	24 min	2.9 (n=4)

For MF6, using six processes (n=6), the runtime was reduced by 59.1% (from 110 min to 45 min), resulting in a speedup of 2.4. For VIC, parallel execution using the RVIC R library with four processes (n=4) achieved a runtime reduction from 69 min to 24 min, yielding a speedup of 2.9. These speedups, achieved without altering model outputs, demonstrate the scalability of both models for large-scale simulations within the VIC-MF6 framework, supporting extended temporal and complex spatial analyses.

However, initial testing revealed limitations in the VIC Classic and RVIC setup. VIC Classic's time-over-space approach, processing all time steps for a single cell before moving to

the next cell, prevented the temporal synchronicity required for integration with MF6, which demands a space-over-time framework. Additionally, RVIC exhibited memory inefficiencies, duplicating input data for each submodel, leading to excessive memory consumption. Trials at 25%, 50%, 75%, and 100% of the full model size showed that RVIC could not support more than three submodels for the full model or six submodels at a 25% scale, with memory usage scaling unfavorably as the submodel count increased. These issues were resolved by transitioning to VIC Image, as described earlier.

3.3.2. Surface Water Hydrology

The VIC model provides an assessment of surface water dynamics in New Mexico from 1990 to 2100, with the period from 1990 to 2023 simulated using observed meteorological forcings and 2024 to 2100 based on CMIP6 forecasted data. The analysis focuses on key hydrologic metrics, including runoff, baseflow, and soil moisture, as detailed below.

Figure 9 illustrates monthly runoff trends over the simulation period, with a 12-month moving average depicted in red. During the observed period (1990–2023), runoff exhibits seasonal variability, peaking during the monsoon months of July and August, with the red moving average highlighting a stable trend over time. In the forecasted period (2024–2100), runoff shows increased seasonal peaks, with the moving average suggesting a gradual upward trend, reflecting potential hydrologic responses to projected climate changes as of August 1, 2025.

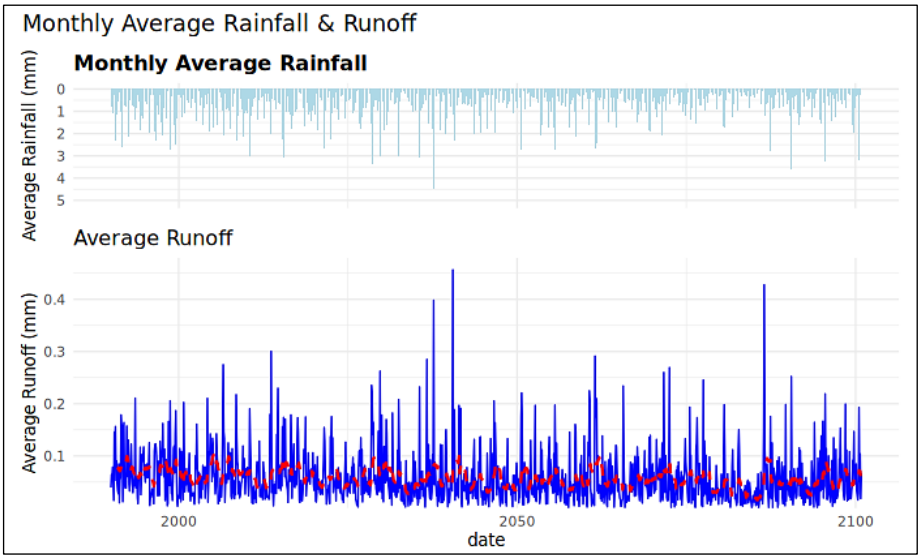

Figure 9. Average Monthly Runoff for the Simulation Period with Monthly 12-Month Moving Average in Red.

Figure 10 details baseflow dynamics. In the observed period, baseflow shows seasonal increases following monsoon rainfall, maintaining a consistent baseline with notable peaks in wet years. The forecasted period indicates a slight rise in baseflow, with sustained elevated levels post-2050, suggesting enhanced groundwater contributions under CMIP6 projections. The sudden peak at the beginning of the forecasted period suggests that the publicly available bias corrected CMIP6 products sometimes require local bias correction to adjust the data as per the local climatic and hydrologic conditions.

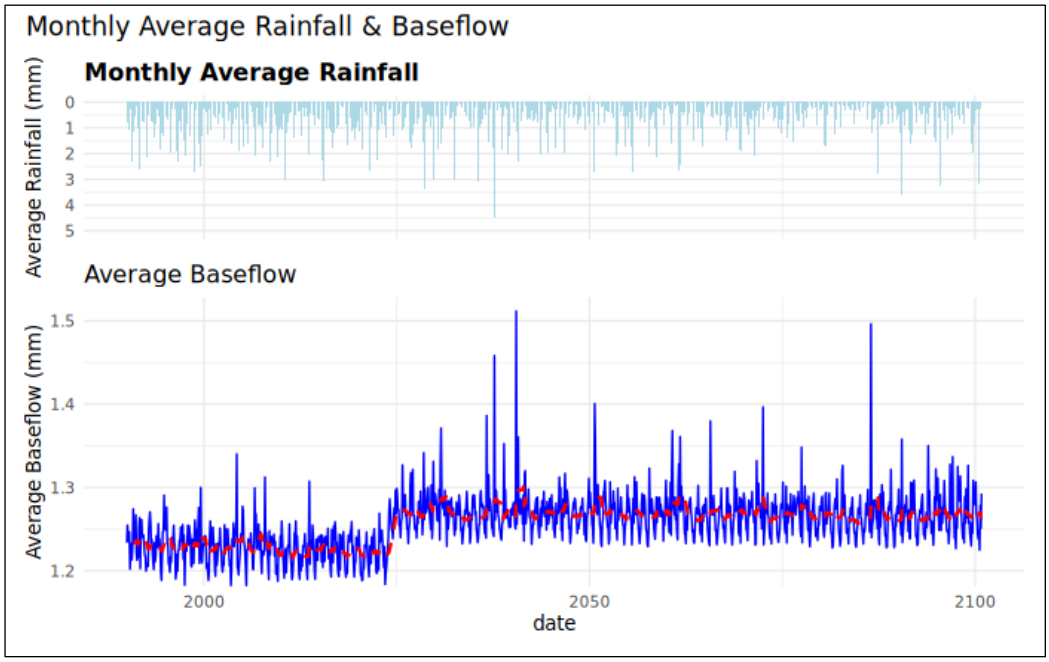

Figure 10. Average Monthly Baseflow for the Simulation Period with Monthly 12-Month Moving Average in Red.

Figure 11 presents soil moisture trends. During the observed period, soil moisture fluctuates with seasonal rainfall, peaking during the monsoon season and stabilizing in drier months. The forecasted period shows a modest increase in peak soil moisture levels, indicating potential changes in water retention capacity through 2100 under forecasted conditions.

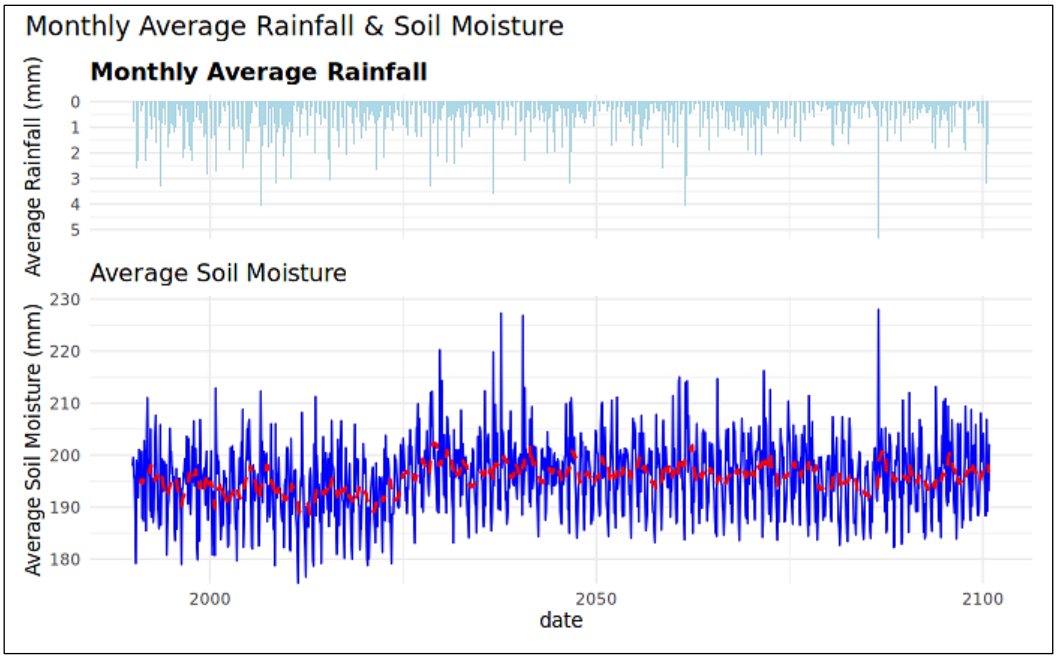

Figure 12. Average Monthly Soil Moisture for the Simulation Period with Monthly 12-Month Moving Average in Red.

Figure 12 shows that the median monthly precipitation is approximately 1.8 mm, with an Interquartile Range (IQR) of 1.2–2.4 mm, reflecting significant seasonal differences. Outliers extend up to 3.0 mm, predominantly during the monsoon months of July and August, indicating occasional high precipitation events. The boxplot suggests a stable baseline with increased variability in the forecasted period, consistent with projected climate trends

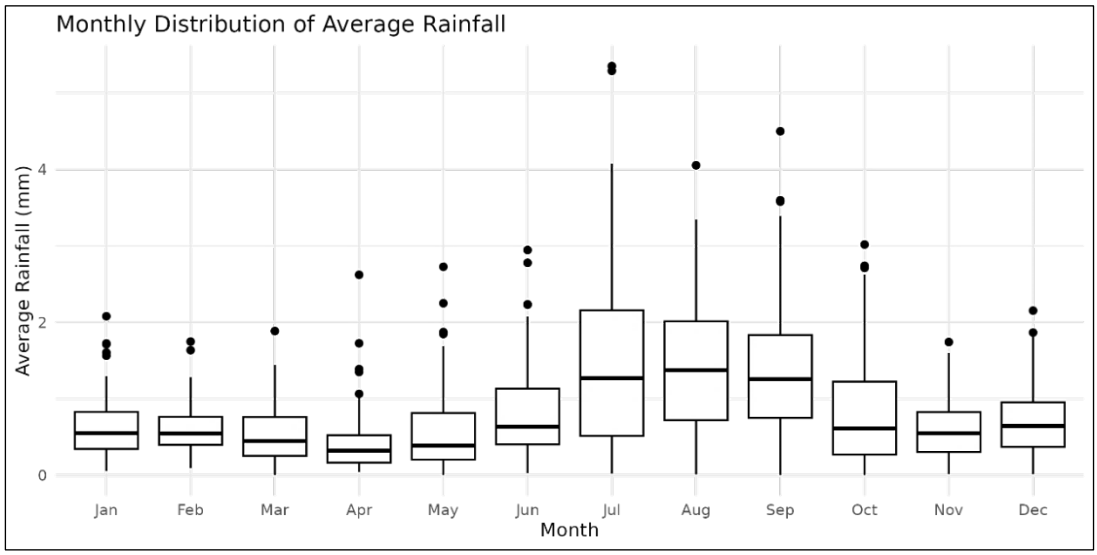

Figure 11. Boxplots of Average Monthly Rainfall.

Figure 13 illustrates the seasonal variability of runoff across the simulation period. The median of statewide monthly average runoff is approximately 0.05 mm, reflecting moderate monthly variation. Outliers extend up to 0.50 mm, predominantly during the monsoon months of July and August, indicating significant seasonal peaks driven by observed and forecasted precipitation patterns.

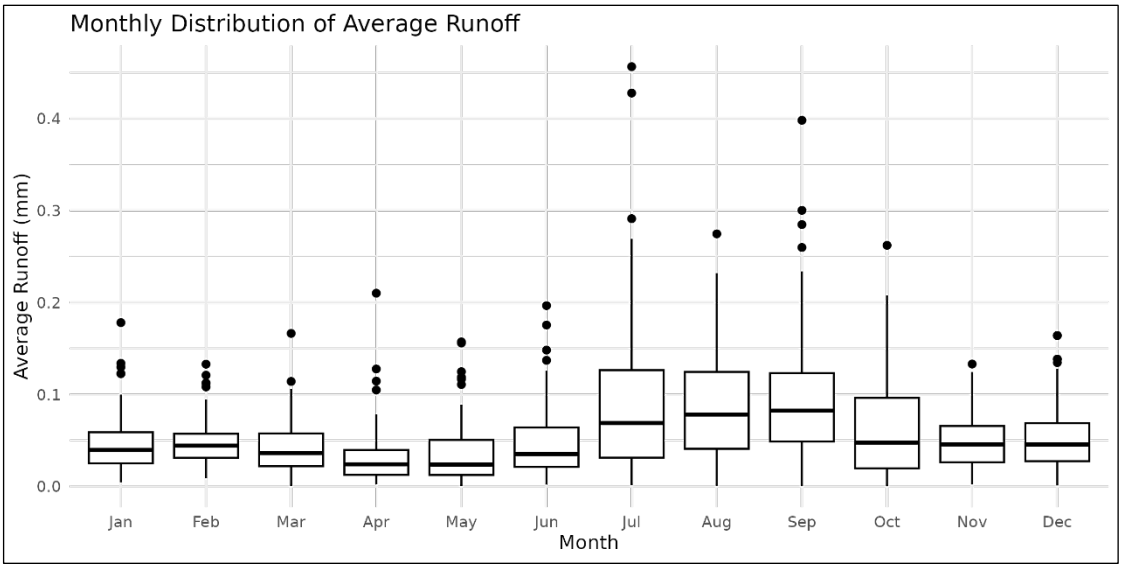

Figure 13. Boxplots of Average Monthly Runoff.

Figure 14 details the monthly dynamics of baseflow. The median baseflow is 1.35 mm, with an IQR of 1.20–1.45 mm, suggesting a stable monthly distribution. Seasonal variations are minimal, with outliers reaching 1.55 mm during wetter months, likely influenced by monsoon recharge and sustained groundwater contributions under CMIP6 projections.

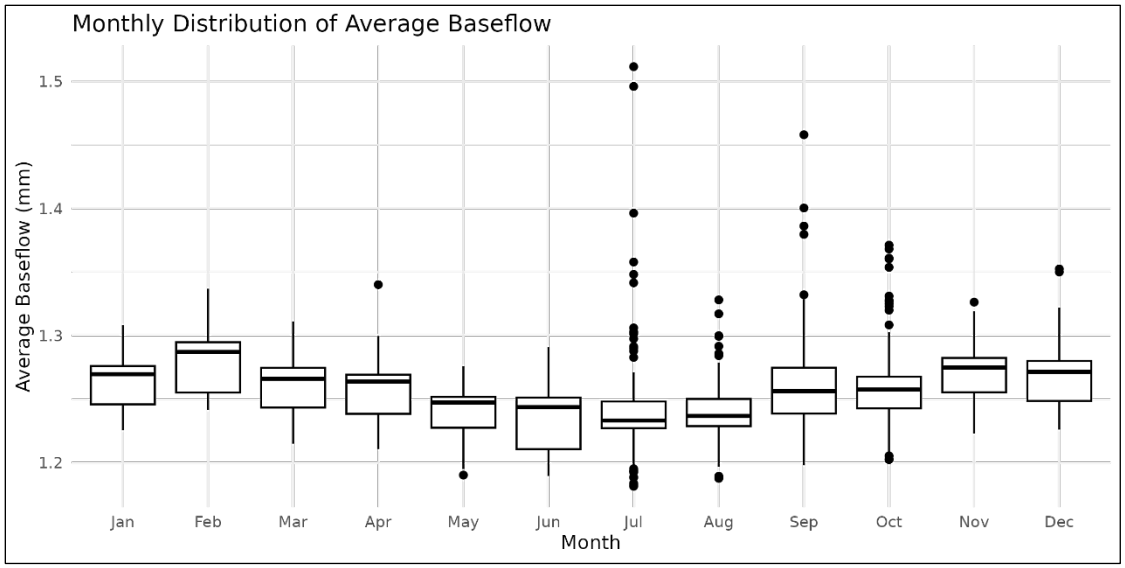

Figure 15. Boxplots of Average Monthly Baseflow.

Figure 15 presents the monthly variability of soil moisture. The median soil moisture is 210 mm, with an IQR of 200–220 mm, indicating a consistent baseline across months. Outliers extend to 230 mm during peak monsoon periods, reflecting increased water retention in response to observed rainfall (1990–2023) and forecasted conditions (2024–2100).

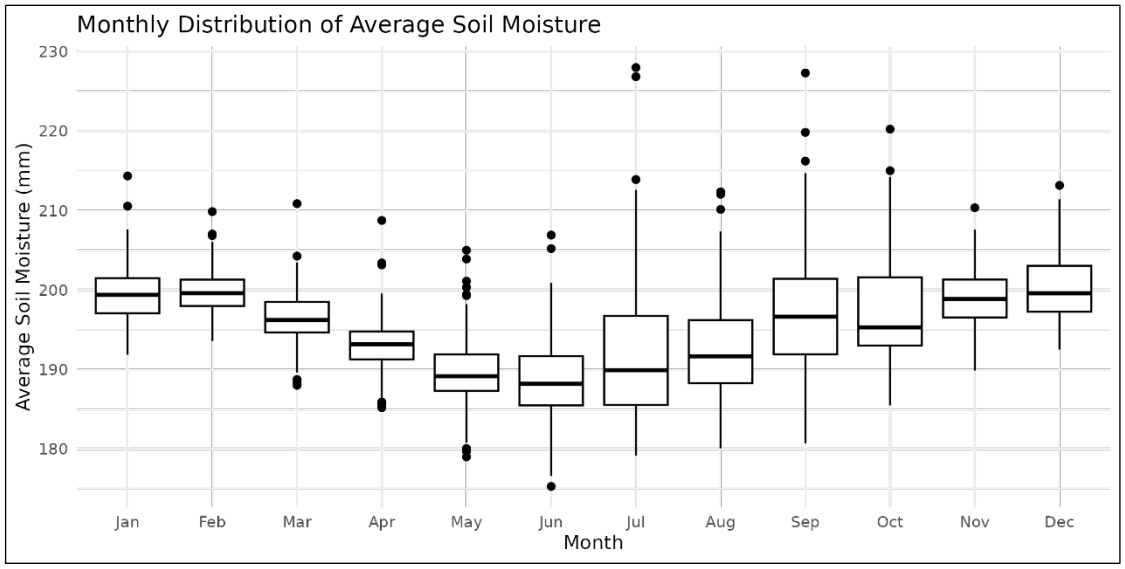

Figure 14. Boxplots of Average Monthly Soil Moisture.

The scatter matrix of average hydrologic metrics in Figure 16 shows that the Average Runoff (ARO) and Baseflow (ABF) are strongly right-skewed, meaning most grid cells have low fluxes and a few have very high values, while the Average Soil Moisture (ASM) follows an approximate normal distribution around 200 mm. All pairwise Pearson correlations are significant ($p < 0.001$): ARO and ABF correlate weakly to moderately ($r = 0.375$), ARO and ASM moderately to strongly ($r = 0.668$), and ABF and ASM strongly ($r = 0.760$). These results reflect VIC's hydrologic behavior where, as soil moisture rises toward saturation, both surface runoff and subsurface flow increase. Scatter in the ARO-ABF relationship indicates additional controls, such as groundwater dynamics affecting baseflow. A clear threshold near 200 mm of ASM marks where runoff begins to increase rapidly, suggests that nonlinear or piecewise regression may better capture runoff generation than a simple linear model. Finally, the strong collinearity between ABF and ASM implies that including both in the same regression could lead to multicollinearity, so dimensionality reduction (for example, principal component analysis) is advisable.

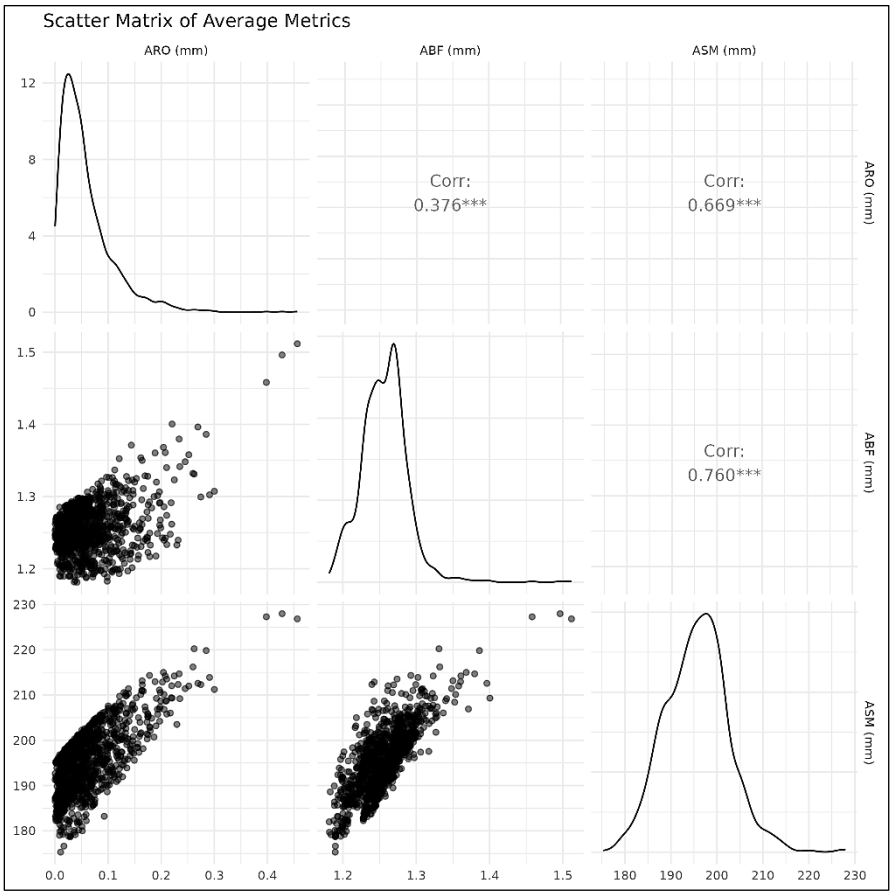

Figure 16. Scatter Matrix of Hydrologic Parameters for New Mexico.

The analysis suggests that the hydrology of New Mexico is dominated by a pronounced seasonal cycle in which modest winter precipitation gives way to a dry spring, followed by the North American Monsoon in midsummer. From December through March, median monthly rainfall lies near 1.2–1.3 mm, sustaining soil moisture at roughly 198–200 mm and baseflow at about 1.25–1.30 mm/month while generating almost no runoff (<0.05 mm). As spring progresses during April–June, soil moisture falls to its annual low (~187–193 mm), baseflow declines to ~1.22–1.25 mm/month, and runoff all but vanishes (<0.03 mm). With the onset of the monsoon during July–September, rainfall surges to 2.0–2.2 mm/month, soil moisture rebounds to 195–198 mm, baseflow increases to 1.28–1.30 mm/month, and surface runoff peaks at 0.10–0.13 mm. These summer pulses are essential for groundwater recharge and streamflow initiation in an otherwise water-limited environment. The strong relationship between soil moisture and baseflow underscores the role of subsurface storage in sustaining flows outside the monsoon period, while the small fraction of precipitation that becomes runoff highlights the dominance of infiltration and evapotranspiration in the regional water balance.

3.3.3. Groundwater Hydrology

The RGTIHM model provides a comprehensive view of groundwater dynamics across the LRG region for the observed period from 1940 (stress period 10) to 2014 (stress period 898), and the forecasted period until 2100 (stress period 1930) with hydraulic head and Water Table Depth (WTD) data evaluated for all the three Stress Periods (SPs) including SP 10 (in the beginning of 1941 after the transient model stabilization) and SP 898, with 2 time steps per SP representing ~15-day time step. The analysis reveals significant spatial and temporal variations across nine layers.

The modeled aquifer system beneath the LRG region exhibits a multilayered flow regime controlled by both regional gradients and localized stresses. As shown in Figure 17, the shallowest layers (Layers 1–3) maintain the highest potentiometric heads (~1,150–1,230 m), reflecting recharge along the mountain front and interaction with surface water in the upstream reaches. Moving downdip through Layers 4–6, median heads decline to ~1,020–1,170 m, illustrating the transition from unconfined to semi-confined conditions and reduced transmissivity in mid-aquifer sands and silts. In the deepest layers (Layers 7–9), heads fall further to 650–1,170 m, consistent with greater confinement, lower hydraulic conductivity, and

longer groundwater travel times toward the distal basin. Table 2 summarizes the heads of individual layers for the three main SPs.

Table 2. Mean Head and Difference in Mean Head for SPs 10, 898, and 1930 for all 9 Layers.

Layer	SP 10	SP 898	SP 1930	SP 898 - SP 10	SP 1930 - SP 10	SP 1930 - SP 898
L1	1177.05	1175.59	1175.12	-1.45	-1.92	-0.47
L2	1171.25	1175.43	1180.78	4.18	9.53	5.35
L3	1231.51	1223.22	1221.4	-8.3	-10.11	-1.82
L4	1180.19	1174.23	1172.74	-5.96	-7.45	-1.49
L5	1129.4	1129.36	1129.33	-0.05	-0.07	-0.02
L6	1084.18	1084.18	1084.37	0	0.2	0.19
L7	1041.75	1041.22	1040.69	-0.53	-1.07	-0.53
L8	997.27	994.8	993.39	-2.47	-3.88	-1.41
L9	943.65	944.45	944.94	0.81	1.3	0.49

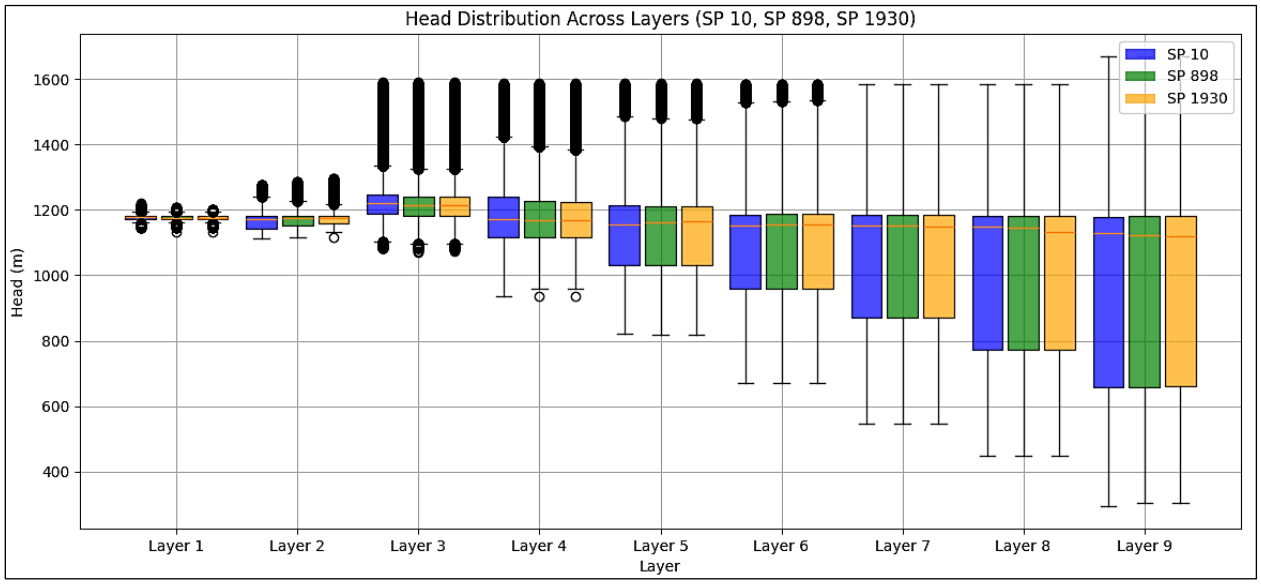

Figure 17. Boxplots of Head Distribution.

Temporal changes in the head reveal both seasonal and long-term responses to irrigation pumping, river recharge, and climatic variability. Figure 18 compares early model spin-up (SP 10) to a mid-simulation period (SP 898), highlighting modest (<50 m) declines along the central valley axis, where pumping stress is greatest. By the end of the simulation (SP 1930), additional drawdown (up to 120 m) appears in the same zones, indicating cumulative depletion under sustained pumping. In contrast, near-river corridors and recharge zones along the mountain front show slight head recovery (5–20 m) during SP 1930, suggesting that monsoon-driven river infiltration partially offsets extraction.

Mid-depth aquifer responses shown in Figure 19 mirror these trends but with attenuated magnitude. Initial drawdown between SP 10 and SP 898 reaches 30–80 m under high-capacity pumping wells. Subsequent comparisons (SP 1930 vs. SP 10) show an additional 40–100 m decline, indicating slower propagation of stress into semi-confined zones. Recovery pockets remain evident near recharge boundaries, consistent with transient river-aquifer exchange during peak runoff months.

The deepest layers shown in Figure 20 exhibit the smallest net changes, with SP 10 to SP 1930 declining generally under 50 m except immediately at the down-gradient of major well fields. This pattern confirms that confined conditions and lower vertical permeability slow both depletion and recovery. Furthermore, seasonal recharge pulses impart negligible fluctuation at depth, reinforcing the notion that long-term pumping is the dominant driver for deep-aquifer head variation.

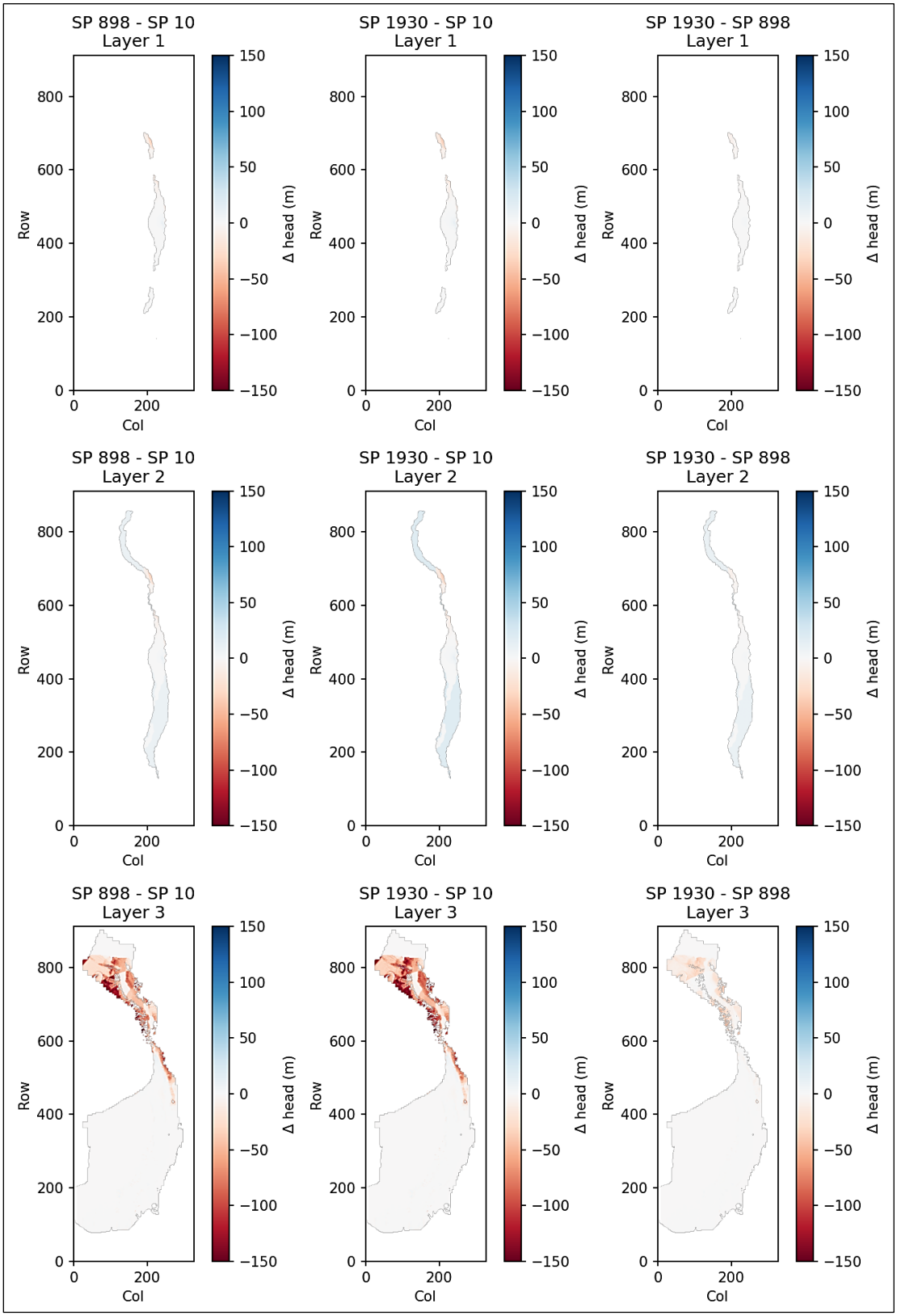

Figure 18. Head Differences Between the Start of Simulation (SP 10), End of Observation (SP 898) and End of Forecasting (SP 1930) for Layers 1–3.

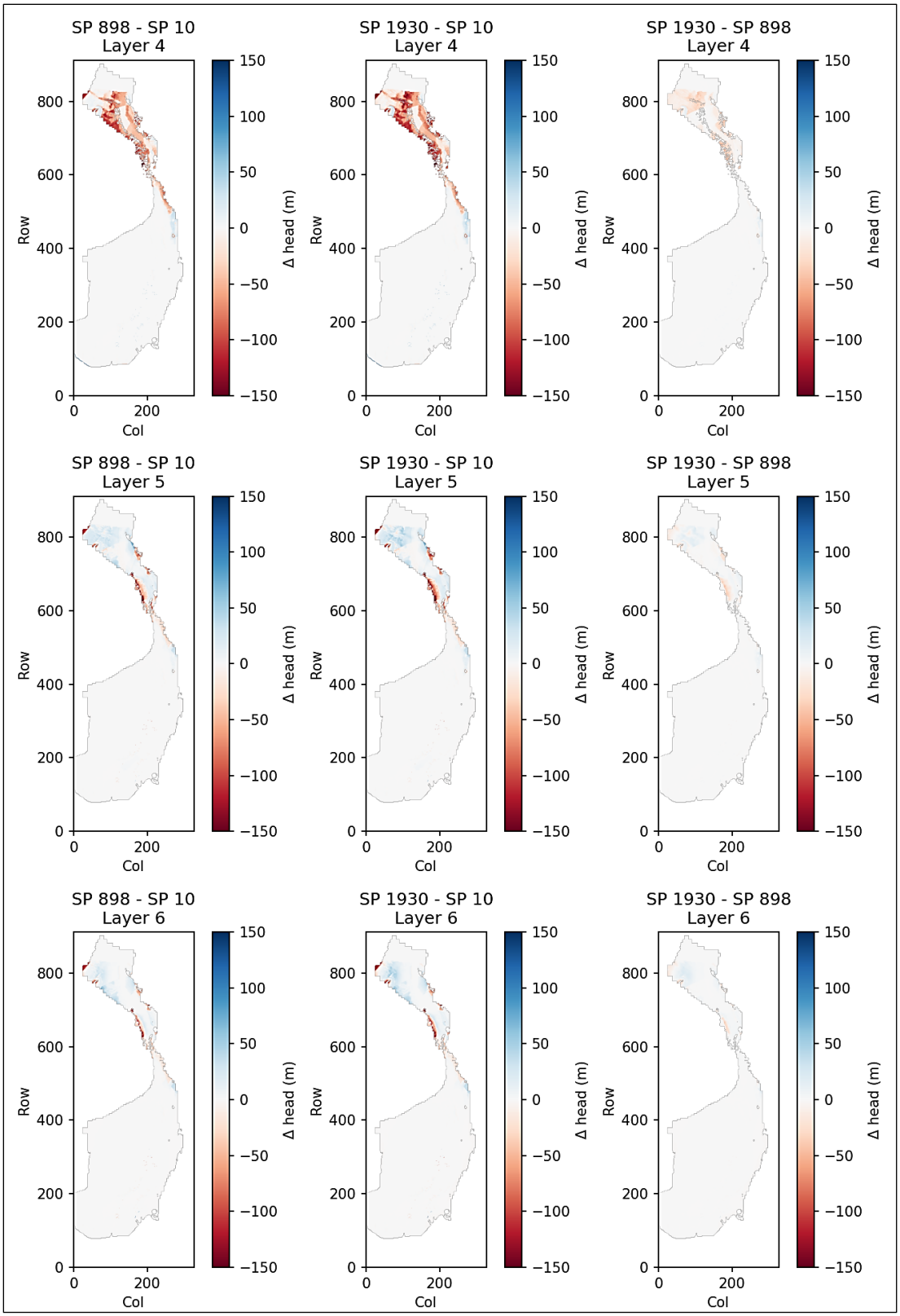

Figure 19. Head Differences Between the Start of Simulation (SP 10), End of Observation (SP 898) and End of Forecasting (SP 1930) for Layers 4–6.

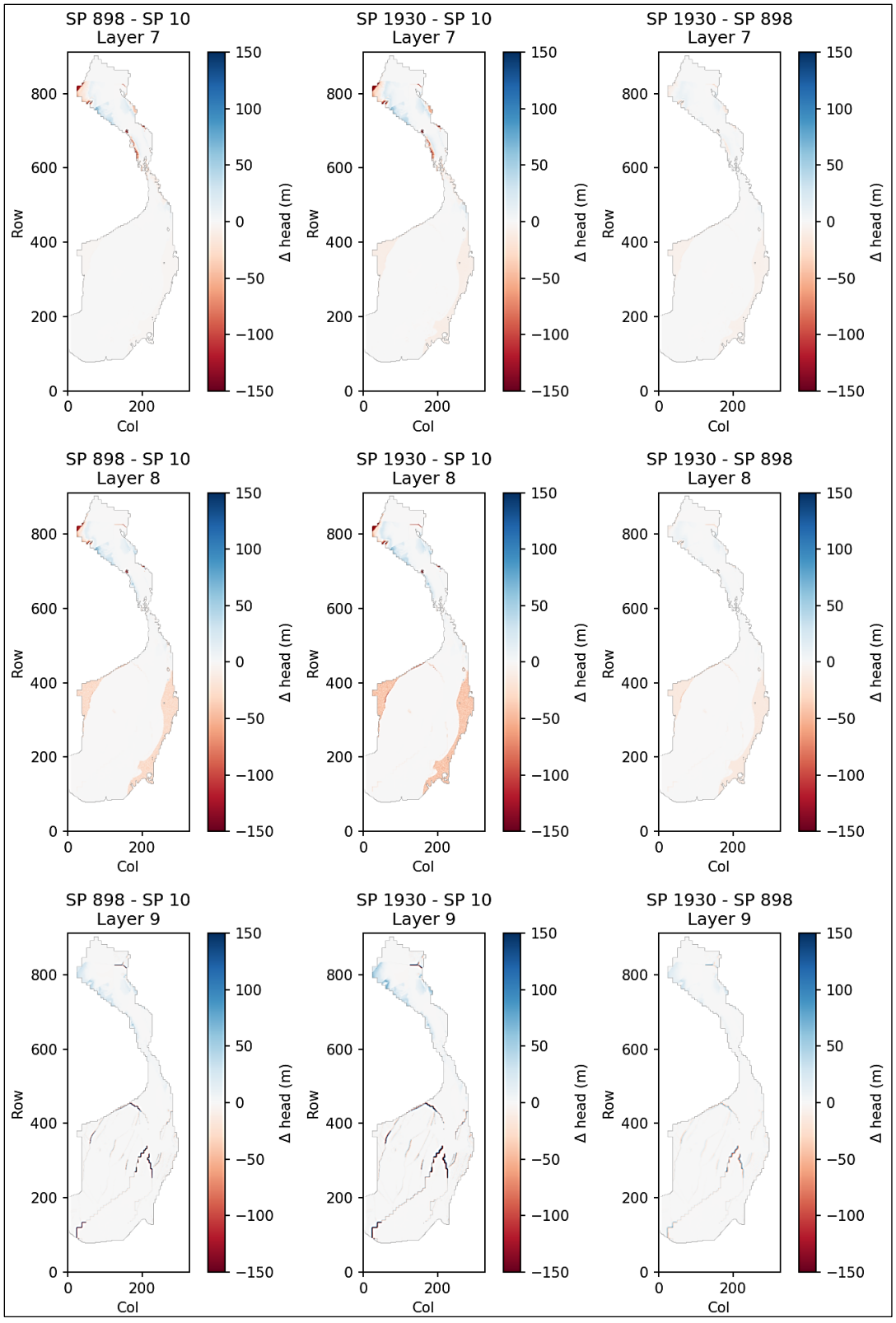

Figure 20. Head Differences Between the Start of Simulation (SP 10), End of Observation (SP 898) and End of Forecasting (SP 1930) for Layers 7–9.

Collectively, these results indicate a strongly anisotropic aquifer system in which shallow unconfined layers respond rapidly to recharge and pumping, while deeper confined units act as a buffer, damping both drawdown and recovery signals. Recharge during the North American Monsoon, modeled via increased river stage and infiltration, produces localized head increases in upgradient areas but does not fully replenish the central valley aquifer under current extraction rates. Management implications include the need for controlled pumping rates to avoid progressive deep-aquifer depletion and the potential benefit of targeted managed aquifer recharge along river corridors to sustain long-term groundwater availability.

4. SOFTWARE ISSUES AND LIMITATIONS

This section summarizes the issues identified in the official MF6 and VIC software, along with potential fixes.

4.1.1. MF6 UZF Package Infiltration Input Overhead

The UZF package incurred significant I/O overhead when coupled with the VIC model, as infiltration was documented as FINF but read as SINF from the package input file. FINF, a state variable, was not accessible via the XMI, requiring internal conversion from SINF to FINF. The MF6 documentation lists FINF as the infiltration variable, but the source code treats it as a hidden state variable and reads it as SINF from the model UZF file. To resolve this, the code was updated to directly read FINF, enabling VIC to pass infiltration as a state variable before each time step. This eliminated excessive file I/O, improving computational efficiency. The resolution is available at: https://github.com/clawrim/modflow6/tree/uzf-fix.

4.1.2. MF6 Bottom Elevation Pass-Through Condition Errors

MF6 exhibited instability in handling pass-through conditions, where cells are marked with IDOMAIN -1. In these cases, the model attempts to identify the bottom elevation (botm) for active cells by finding the top elevation from the layer above. However, the internal routine performs only a single upward check. If the immediate layer above is inactive or missing, the model fails to find a valid top and terminates with an error.

This limitation becomes critical in models like RGTIHM, where many geologic layers may contain gaps, Not-a-Number (NaN) values, or represent units that do not exist uniformly across the model domain. For example, in areas where Base_BSMT is the only present layer, for MF6,

it may lie several layers below the nearest valid surface, with all intermediate layers being pass-through cells. In such configurations, the default logic fails to identify a valid top elevation, leading to incorrect top-bottom pairing or model crashes.

To resolve this issue, we implemented an enhanced loop that searches iteratively upward through the layer stack until a valid top is found. This valid top may come from either a non-pass-through geologic layer or the surface elevation defined by the Digital Elevation Model (DEM). By continuing the search instead of stopping at the first invalid result, the model can now assign correct top and bottom elevations even in structurally complex regions. The resolution is available at: https://github.com/clawrim/modflow6/tree/dis-fix. This resolution enhances MF6's reliability and efficiency in the coupled framework, supporting accurate hydrologic simulations.

4.1.3. MF6 Revised Indexing

Mid-study, we discontinued the MRG Basin Model because of significant challenges in converting from MF2K to MF6. The primary issue stemmed from MF6's reversed indexing system. Unlike MF2K and MF5, where the (0,0) coordinate corresponds to the upper-left corner (xul, yul), MF6 designates (0,0) as the lower-left corner (xll, yll). During the intermediate conversion through MF5, this shift caused the MRG Basin model to fail to converge. The input data, aligned with the older indexing, became misaligned with MF6's grid, and when combined with the applied IDOMAIN mask, the data went out of bounds, leading to model collapse. To include the MRG model, we either need to fix the MF5to6 converter or change the whole MRG model configuration.

4.1.4. NetCDF Format Conflict Between VIC and Standard Libraries

A notable compatibility issue arose during the integration of VIC with MF6, stemming from a mismatch in NetCDF file formats. The Xarray library, which relies on h5netcdf or netCDF4 Python libraries, performs optimally with NetCDF-4 files that use an HDF5 backend, making NetCDF-4 the preferred format for advanced data structures. However, VIC, by default, generates outputs in NetCDF-3 Classic or NetCDF-4 Classic format, depending on the linked NetCDF library, lacking features like compression or large file support that are available in full NetCDF-4. This format discrepancy led to errors in the coupling process, as Xarray expects NetCDF-4/HDF5, while VIC produced NetCDF-3 Classic files. Specifically, when Xarray

attempted to read or write these files, it altered the file's magic bytes, resulting in "permission denied" or "file corruption" errors. This issue is exacerbated by insufficient documentation in both VIC and Xarray regarding format compatibility, increasing the risk of I/O failures.

The resolution involved updating the VIC converter to explicitly output NetCDF-4 (HDF5-backed) files, ensuring seamless compatibility with Xarray and preventing file corruption during I/O operations. This fix underscores the importance of aligning file formats in coupled modeling workflows to avoid runtime exceptions and ensure robust data handling.

4.1.5. Issues in Parallel Execution of the Framework

4.1.5.1. VIC Image Driver Parallelization Issue. The VIC model employs hybrid OpenMP and MPI parallelization, but the VIC Image Driver has an incomplete OpenMP implementation, causing data races when run with multiple processing threads (any environment variable other than OMP_NUM_THREADS=1). The fix requires a revised OpenMP implementation to ensure stable hybrid parallel execution, which is currently under development.

4.1.5.2. METIS Optimized Splitting and MF6 Splitter Limitation. The MF6 splitter cannot handle models with Horizontal Flow Barriers (HFB) in parallel, a significant limitation for the RGTIHM, which extensively uses HFB. Currently, splitting the model into submodels results in imbalanced computational loads, reducing parallel efficiency. Alternatives include either accepting the imbalance or implementing HFB splitting in the MF6 splitter. Because of these unresolved issues, the framework remains sequential in nature as of now, pending further development to enable efficient parallel execution. These resolutions and ongoing efforts to address parallel execution challenges are expected to enhance the VIC-MF6 framework's reliability, supporting accurate and efficient hydrologic simulations across New Mexico.

4.1.5.3. Coupled Calibration and Bias Correction. This study focused on building a coupled surface-subsurface hydrologic modeling framework and validating the coupling processes. While the surface water and groundwater models were previously calibrated independently, the coupled system may still require joint recalibration and further validation of hydrologic outputs. Additionally, because of a lack of complete observed data for certain forcing variables, two different climate models were used for meteorological forcing: MTCLIM (as suggested by the VIC documentation) for the historical period and CMIP6 for the future projections. This use of

two different models for the unobserved forcing variables resulted in some inconsistencies between the two simulation periods, which are reflected in the baseflow and soil moisture trends.

5. FUTURE WORK

Our future work involves further validation and refinement of the coupled hydrologic outputs to support statewide drought vulnerability analysis, potentially through recalibration of the coupled model. Recalibration may be necessary because the original surface and groundwater models were independently calibrated without accounting for the interactions introduced through coupling. Validation against historical observations will ensure accuracy, particularly for extreme events like droughts and floods. Subsequently, we will develop a drought vulnerability index for the entire state of New Mexico, leveraging the coupled model's outputs to assess spatial and temporal risks under both historical and projected climate scenarios (up to 2100). Additionally, we plan to address issues in the MF2K MRG model, focusing on updating its grid structure, boundary conditions, and calibration to align with modern standards, and then integrate it into our framework alongside the RGTIHM. This incorporation of the new groundwater model into the currently coupled model will expand the modeling region for a more comprehensive statewide hydrologic analysis.

For future enhancements to the VIC-MF6 framework, we will focus on improving its scalability and applicability for statewide water resources management by implementing parallel simulations of both VIC and MF6 submodels within the coupled modeling framework. Following parallelization, the framework will be calibrated on HPC using historical data from 1940 to 2023 to optimize model parameters. Additionally, to address the discrepancy issue in the baseflow and soil moisture results between the two historical and forecasting simulation periods, we suggest the correction of systemic bias in both modeled weather-forcing variables.

6. CONCLUSIONS

This study presents a fully functional coupled modeling framework linking the VIC Image Driver and MF6 for statewide hydrologic simulation in New Mexico. The system runs from 1990 to 2100, capturing surface and groundwater interactions at a resolution of 1/32° and across nine vertical geologic layers. Model integration resolved major technical issues, including NetCDF format mismatch, problems with UZF infiltration input in MF6, and incorrect handling of

vertical pass-through cells, which required source code modifications. The coupled model produces key hydrologic signals. VIC outputs show seasonal soil moisture ranging from 185 mm to 230 mm and monsoon-driven runoff peaking at 0.13 mm/month. The median baseflow is stable around 1.35 mm/month with low variability. MF6 results show cumulative groundwater drawdown up to 120 m in shallow layers from 1940 to 2100, with a mean head decline of 10.1 m in Layer 3 and local recovery near river corridors. Deeper layers (7–9) remain largely stable, with changes under 3 m. These results confirm that the framework captures both short-term hydrologic variability and long-term groundwater trends. It is ready for scenario testing, climate impact analysis, and sustainable water planning across arid basins. Future work will focus on joint calibration, local climate bias correction, and expanding parallel capabilities.

SOFTWARE AND DATA AVAILABILITY

The source code and programs are available at

- https://github.com/clawrim/vic-mf6,
- https://github.com/clawrim/vic-classic-to-image,
- https://github.com/clawrim/modflow6, and
- https://github.com/clawrim/rgtihm.

The model files and data will be provided upon request because of their large size.

ACKNOWLEDGMENTS

The research on which this report is based was financed in part by the U.S. Department of the Interior, Geological Survey, through the New Mexico Water Resources Research Institute. This material is based upon work supported by the U.S. Geological Survey under Grant/Cooperative Agreement No. G21AP10635, along with additional funding by the New Mexico Legislature, through the NM WRRI.

REFERENCES

Abatzoglou, J.T. (2013). Development of gridded surface meteorological data for ecological applications and modelling. Int. J. Climatol., 33: 121–131.

Arnold, J.G., Srinivasan, R., Muttiah, R.S., & Williams, J.R. (1998). Large area hydrologic modeling and assessment part I: model development 1. JAWRA Journal of the American Water Resources Association, 34(1), 73–89.

Eyring, V., Bony, S., Meehl, G.A., Senior, C.A., Stevens, B., Stouffer, R.J., & Taylor, K.E. (2016). Overview of the Coupled Model Intercomparison Project Phase 6 (CMIP6) experimental design and organization, Geosci. Model Dev., 9, 1937-1958, doi:10.5194/gmd-9-1937-2016, 2016.

Forum, M.P. (1994). *MPI: A message-passing interface standard*. University of Tennessee.

Gutjahr, O., Putrasahan, D., Lohmann, K., Jungclaus, J.H., von Storch, J.-S., Brüggemann, N., Haak, H., & Stössel, A. (2019). Max Planck Institute Earth System Model (MPI-ESM1.2) for the High-Resolution Model Intercomparison Project (HighResMIP), Geosci. Model Dev., 12, 3241–3281, https://doi.org/10.5194/gmd-12-3241-2019.

Hamman, J.J., Nijssen, B., Bohn, T.J., Gergel, D.R., & Mao, Y. (2018). The Variable Infiltration Capacity model version 5 (VIC-5): Infrastructure improvements for new applications and reproducibility. Geoscientific Model Development, 11(8), 3481–3496.

Hanson, R.T., Ritchie, A.B., Boyce, S.E., Galanter, A.E., Ferguson, I.A., Flint, L.E., Flint, A.L., & Henson, W.R. (2020). *Rio Grande transboundary integrated hydrologic model and water-availability analysis, New Mexico and Texas, United States, and northern Chihuahua, Mexico*. US Geological Survey. https://doi.org/10.3133/sir20195120.

Hughes, J.D., Russcher, M.J., Langevin, C.D., Morway, E.D., & McDonald, R.R. (2022). The MODFLOW Application Programming Interface for simulation control and software interoperability. Environmental Modelling & Software, 148, 105257.

Hungerford, R.D., Nemani, R.R., Running, S.W., & Coughlan, J.C. (1989). MTCLIM: a mountain microclimate simulation model. Res. Pap. INT-RP-414. Ogden, UT: U.S. Department of Agriculture, Forest Service, Intermountain Research Station. 52 p.

Hutton, E.W.H., Piper, M.D., & Tucker, G.E. (2020). The Basic Model Interface 2.0: A standard interface for coupling numerical models in the geosciences. Journal of Open Source Software, 5(51), 2317, https://doi.org/10.21105/joss.02317.

IEEE (2024). IEEE Std 1003.1-2024 (The Open Group Base Specifications Issue 8): Portable Operating System Interface (POSIX). IEEE Computer Society.

Jafari, T., Kiem, A.S., Javadi, S., Nakamura, T., & Nishida, K. (2021). Fully integrated numerical simulation of surface water-groundwater interactions using SWAT-MODFLOW with an improved calibration tool. Journal of Hydrology: Regional Studies, 35, 100822.

Ketchum, D. G. (2016). *High-resolution estimation of groundwater recharge for the entire state of New Mexico using a soil-water-balance model*. New Mexico Institute of Mining and Technology.

Langevin, C.D., Hughes, J.D., Banta, E.R., Provost, A.M., Niswonger, R.G., & Panday, S. (2017). MODFLOW 6 modular hydrologic model: US Geological Survey Software. US Geological Survey.

Liang, X., Lettenmaier, D.P., Wood, E.F., & Burges, S.J. (1994). A simple hydrologically based model of land surface water and energy fluxes for general circulation models. Journal of Geophysical Research: Atmospheres, 99(D7), 14415–14428.

Maurer, E.P., Wood, A.W., Adam, J.C., Lettenmaier, D.P., & Nijssen, B. (2002). A long-term hydrologically based dataset of land surface fluxes and states for the conterminous United States. Journal of Climate, 15(22), 3237–3251.

McAda, D.P., & Barroll, P. (2002). *Simulation of ground-water flow in the Middle Rio Grande basin between Cochiti and San Acacia, New Mexico* (Vol. 2, Issue 4200). US Department of the Interior, US Geological Survey.

Neteler, M., Bowman, M.H., Landa, M., & Metz, M. (2012). GRASS GIS: A multi-purpose open source GIS. Environmental Modelling & Software, 31, 124–130.

National Oceanic and Atmospheric Administration (NOAA), (1976). *US Standard Atmosphere, 1976* (NOAA-S/T-76-1562).

PRISM Group (2014), Oregon State University, https://prism.oregonstate.edu, data created February 4, 2014, accessed July 31, 2025.

Sridhar, V., Billah, M.M., & Hildreth, J.W. (2018). Coupled surface and groundwater hydrological modeling in a changing climate. Groundwater, 56(4), 618–635.

Sweetkind, D.S. (2017). *Three-dimensional hydrogeologic framework model of the Rio Grande transboundary region of New Mexico and Texas, USA, and northern Chihuahua, Mexico*. US Geological Survey.

Union of Concerned Scientists (UCS). (2016). *Confronting Climate Change in New Mexico*. 1–14.

Xu, F. (2018). *Estimation of focused recharge for New Mexico using a soil-water-balance model: PyRANA*. New Mexico Institute of Mining and Technology.

Yang, Y., Pan, M., Beck, H.E., Fisher, C.K., Beighley, R.E., Kao, S., Hong, Y., & Wood, E.F. (2019). In quest of calibration density and consistency in hydrologic modeling: Distributed parameter calibration against streamflow characteristics. Water Resources Research, 55(9), 7784–7803.

New Mexico Water Resources Research Institute
3170 S. Espina Street
New Mexico State University
Las Cruces, NM 88003-8001

(575) 646-4337 • nmwrri@nmsu.edu